STRESS-STRAIN MODEL OF UNCONFINED AND CONFINED CONCRETE AND STRESS-BLOCK PARAMETERS

A Thesis

by

MADHU KARTHIK MURUGESAN REDDIAR

Submitted to the Office of Graduate Studies of
Texas A&M University
in partial fulfillment of the requirements for the degree of

MASTER OF SCIENCE

December 2009

Major Subject: Civil Engineering

STRESS-STRAIN MODEL OF UNCONFINED AND CONFINED CONCRETE AND STRESS-BLOCK PARAMETERS

A Thesis

by

MADHU KARTHIK MURUGESAN REDDIAR

Submitted to the Office of Graduate Studies of
Texas A&M University
in partial fulfillment of the requirements for the degree of

MASTER OF SCIENCE

Approved by:

Chair of Committee,	John B. Mander
Committee Members,	Mohammed E. Haque
	Monique Hite Head
Head of Department,	John Niedzwecki

December 2009

Major Subject: Civil Engineering

ABSTRACT

Stress-Strain Model of Unconfined and Confined Concrete and Stress-Block Parameters.

(December 2009)

Madhu Karthik Murugesan Reddiar, B-Tech., Pondicherry Engineering College,

Puducherry, India

Chair of Advisory Committee: Dr. John B. Mander

Stress-strain relations for unconfined and confined concrete are proposed to overcome some shortcomings of existing commonly used models. Specifically, existing models are neither easy to invert nor integrate to obtain equivalent rectangular stress-block parameters for hand analysis and design purposes. The stress–strain relations proposed are validated for a whole range of concrete strengths and confining stresses. Then, closed form expressions are derived for the equivalent rectangular stress-block parameters. The efficacy of the results is demonstrated for hand analysis applied for deriving the moment-curvature performance of a confined concrete column. Results are compared with those obtained from a computational fiber-element using the proposed stress-strain model and another widely used model; good agreement between the two is observed. The model is then utilized in the development of a new structural system that utilizes the positive attributes of timber and concrete to form a parallel. Timber has the advantage of being a light weight construction material, easy to handle, is environmentally friendly. However, large creep deflections and significant issues with sound transmission (the footfall problem) generally limit timber use to small spans and

low rise buildings. Concrete topping on timber sub-floors mitigate some of these issues, but even with well engineered wood systems, the spans are relatively short. In this study, a new structural system called *structural boxed-concrete*, which utilizes the positive attributes of both timber and reinforced concrete to form a parallel system (different from timber-concrete composite system) is explored. A stress-block approach is developed to calculate strength and deformation. An analytical stress-block based moment-curvature analysis is performed on the timber-boxed concrete structural elements. Results show that the structural timber-boxed concrete members may have better strength and ductility capacities when compared to an equivalent ordinary reinforced concrete member.

DEDICATION

To my Father and Mother

ACKNOWLEDGEMENTS

I thank my committee chair, Dr. Mander for his invaluable guidance and support throughout the course of this research. This work would not have been possible without his vision, thoughts and financial support.

I would also like to thank Dr. Head and Dr. Haque for serving on my advisory committee. Thanks also to the department faculty and staff for making my time at Texas A&M University a great and memorable experience. I would also like to thank my friends at Texas A&M University and elsewhere for their constant support and encouragement.

Last, but not the least I would like to show my gratitude towards my parents and brother for making this unforgettable journey at Texas A&M University possible and for their constant support, prayers and encouragement.

TABLE OF CONTENTS

Page

Page

LIST OF FIGURES

Page

LIST OF TABLES

Page

1. INTRODUCTION

1.1 Research Motivation

Several models for the stress-strain relation of concrete have been proposed in the past. Although the behavior of concrete up to the maximum concrete strength is well established, the post-peak branch and the behavior of high-strength concrete has been an area of extensive research more recently.

Another area which has seen much research is in establishing a good stress-strain relation for confined concrete. Confinement in concrete is achieved by the suitable placement of transverse reinforcement. At low levels of stress, transverse reinforcement is hardly stressed; the concrete behaves much like unconfined concrete. At stresses close to the uniaxial strength of concrete internal fracturing causes the concrete to dilate and bear out against the transverse reinforcement which then causes a confining action in concrete. This phenomenon of confining concrete by suitable arrangement of transverse reinforcement causes a significant increase in the strength and ductility of concrete. The enhancement of strength and ductility by confining the concrete is an important aspect that needs to be considered in the design of structural concrete members especially in areas prone to seismic activity, blast effects or vehicle crashes. Again, several models are available for the stress-strain relation of confined concrete.

This thesis follows the style of *Journal of Structural Engineering.*

With the advent of high strength concrete in the early 1970's, its use has increased significantly over the years. In the present day scenario high-strength concrete is extensively used in the construction of bridges, high rise buildings, precast and prestressed concrete members and many other structures. With every passing decade the maximum compressive strength of concrete that has been attained has been increasing. Apart from having a higher strength, high strength concrete exhibits a brittle behavior as compared to normal strength concrete. Brittle failure of concrete structural members is a characteristic that is least desired in any kind of structure as it leads to the sudden collapse of structures leading to damage and loss of property and life. These characteristics of high-strength concrete that make them different from those of normal-strength concrete make it important to study their behavior in order to get a good estimate of the strength and ductility capacities of the structural members that are constructed using high strength concrete.

Shortcomings exist when manipulating the most commonly used existing stress-strain models. First, the equations cannot be easily inverted to explicitly calculate strain as a function of stress; this poses a problem when one wants to conduct rate-dependant modeling. Second, the equations cannot be easily integrated in order to determine the equivalent rectangular stress-block parameters for hand analysis and design purposes.

Although the stress-strain models proposed by various researchers have varying levels of sophistication, for the best models it is difficult to check their accuracy. There is a need for a well developed stress-strain model that can not only be used

computationally, but can also be easily adapted for hand analysis to enable rapid design checks to be performed.

This research aims at utilizing the best attributes of earlier models and proposes a new stress-strain model for concrete that represents the properties of both unconfined and confined concrete and at the same time is simple, such that it can be easily inverted and integrated to determine the equivalent rectangular stress-block parameters for unconfined and confined concrete.

The present study also presents a conceptual idea of using timber and reinforced concrete in a parallel system (unlike the composite timber-concrete system) called the *structural timber-concrete system*. This system utilizes the positive aspects of both timber and concrete as individual materials and does not rely on their composite action and hence does not have any detailed connection requirements. Specifically, the concept is based in the formation of the two main elements of construction: beams (and of course the slabs they support) and columns. Another purpose of this study is to reinvigorate the use of common dimension lumber into economical moment frame construction and also to provide the illusion that the building, although quite tall, is really timber. Concrete is used to strengthen, lengthen and stiffen the mostly timber members. One of the main attributes of timber, its lightness, can essentially be maintained.

1.2 Problem Statement

In order to study the behavior of normal or high strength concrete, one of the most important steps is to establish appropriate analytic stress-strain models that capture

the real (observable) behavior. The better the stress-strain model, the more reliable is the estimate of strength and deformation behavior of concrete structural members.

Another important characteristic of concrete is that it exhibits different behavior in its confined and unconfined states. Apart from higher strength, confined concrete tends to show a much greater ductility when compared to unconfined concrete. Thus, it becomes important and desirable to have a stress-strain model that differentiates the behavior of confined and unconfined concrete.

In the absence of sufficient test data it becomes important to have some guidelines or empirical relations to determine the parameters that are required to establish a representative stress-strain relation. This study also aims in identifying the most important parameters and establishing empirical relations for these parameters that are required to define generalized stress-strain relations for concrete.

Another important concept in the analysis and design of concrete structures is the use of equivalent rectangular stress-block parameters. Stress-block analysis has been used in hand computations for defining the nominal strength for the design of reinforced concrete sections. However, this concept can be extended for other strain profiles and limit states. Hence, it is important to be able to derive generalized expressions for the equivalent rectangular stress-block parameters for both confined and unconfined concrete from their respective stress-strain relations. Determining closed form relations for the stress-block parameters for unconfined and confined concrete makes it possible

to apply them in both hand and computer analysis to determine a moment-curvature relationship for a specific structural concrete members.

1.3 Research Objective

The major objectives of the research are outlined below:

i. To establish a stress-strain model of concrete that can well represent the overall stress-strain behavior of normal strength and high strength concrete with a good control over the ascending and descending branches.

ii. To develop stress-strain models that represents the behavior of confined and unconfined concrete.

iii. To develop empirical relations based on the compressive strength of concrete for the parameters that drive the stress-strain relation of both unconfined and confined concrete.

iv. To obtain closed form equations for the stress-block parameters - the effective average concrete stress ratio (α) and the effective stress-block depth factor (β) – so that they can be used to determine the strength and curvature capacity of structural concrete members. The equations for these parameters need to be established for both confined and unconfined concrete.

v. To determine the moment-curvature relation for a reinforced concrete column using the proposed stress-strain relation by fiber analysis and also by hand computations using the equivalent rectangular stress-block parameters and compare the results.

vi. To conceptually develop a system of structural timber-boxed concrete and compare their moment capacities with normally reinforced concrete sections.

vii. To extend the concept of the proposed stress-strain model for unconfined concrete to timber in order to be able to calculate the moment capacity of timber-boxed concrete sections.

viii. To develop equivalent rectangular stress-block parameters for timber in order to extend the concept of stress-block analysis to timber for the analysis and design of timber structural members.

1.4 Review of Previous Relevant Rule-Based Constitutive Models

The investigation into the stress-strain relation of unconfined and confined concrete has been a topic of research for a several years. A brief review of the models that are considered to be important building blocks for the present study are reviewed in this section.

UNCONFINED CONCRETE

Kent and Park (1971) proposed a stress-strain equation for both unconfined and confined concrete. In their model they generalized Hognestad's (1951) equation to more completely describe the post-peak stress-strain behavior. In this model the ascending branch is represented by modifying the Hognestad second degree parabola by replacing 0.85 f_c' by f_c' and ε_{co} by 0.002.

$$f_c = f_c' \left[\frac{2\varepsilon_c}{\varepsilon_{co}} - \left(\frac{\varepsilon_c}{\varepsilon_{co}} \right)^2 \right] \quad (1)$$

The post-peak branch was assumed to be a straight line whose slope was defined primarily as a function of concrete strength.

$$f_c = f_c'[1 - Z(\varepsilon_c - \varepsilon_{co})] \tag{2}$$

in which

$$Z = \frac{0.5}{\varepsilon_{50u} - \varepsilon_{co}} \tag{3}$$

where ε_{50u}= the strains corresponding to the stress equal to 50% of the maximum concrete strength for unconfined concrete.

$$\varepsilon_{50u} = \frac{3 + 0.29f_c'}{145f_c' - 1000} \ (f_c' \ in \ MPa)$$
$$\varepsilon_{50u} = \frac{3 + 0.002f_c'}{f_c' - 1000} \ (f_c' \ in \ Psi) \tag{4}$$

The Kent and Park model is represented in Figure 1a.

Popovics (1973) proposed a single equation to describe unconfined concrete stress-strain behavior. A major appeal of this model is that it only requires three parameters to control the entire pre and post peak behavior, specifically f_c', ε_{co} and E_c.

$$\frac{f_c}{f_c'} = \frac{n\left(\frac{\varepsilon_c}{\varepsilon_{co}}\right)}{(n-1) + \left(\frac{\varepsilon_c}{\varepsilon_{co}}\right)^n} \tag{5}$$

in which the power '*n*' can be expressed as an approximate function of the compressive strength of normal-weight concrete as

$$n = 0.4 \times 10^{-3} f_c'(psi) + 1.0 \tag{6}$$

Popovics equation works well for most normal strength concrete ($f_c' < 55Mpa$), but it lacks the necessary control over the slope of the post-peak branch for high strength concrete.

Thorenfeldt et al. (1987) made modifications to the Popovics (1973) relation to adjust the descending branch of the concrete stress-strain relation. The authors proposed the following equation for the unconfined concrete stress-strain relation.

$$\frac{f_c}{f_c'} = \frac{n\left(\frac{\varepsilon_c}{\varepsilon_{co}}\right)}{(n-1) + \left(\frac{\varepsilon_c}{\varepsilon_{co}}\right)^{nk}} \tag{7}$$

In the above equation '*k*' takes a value of 1 for values of $\left(\frac{\varepsilon_c}{\varepsilon_{co}}\right) < 1$ and values greater than 1 for $\left(\frac{\varepsilon_c}{\varepsilon_{co}}\right) > 1$. Thus by adjusting the value of '*k*' the post-peak branch of the stress-strain relation can be made steeper. This approach can be used for high-strength concrete where the post-peak branch becomes steeper with increase in the concrete compressive strength.

Tsai (1988) proposed a generalized form of the Popovics (1973) equation which has greater control over the post-peak branch of the stress-strain relation. Tsai's equation consists of two additional parameters, one to control the ascending and a second to control the post-peak behavior of the stress-strain curve. The proposed stress-strain relation for unconfined concrete by Tsai is

$$y = \frac{mx}{1 + \left(m - \frac{n}{n-1}\right)x + \frac{x^n}{n-1}} \tag{8}$$

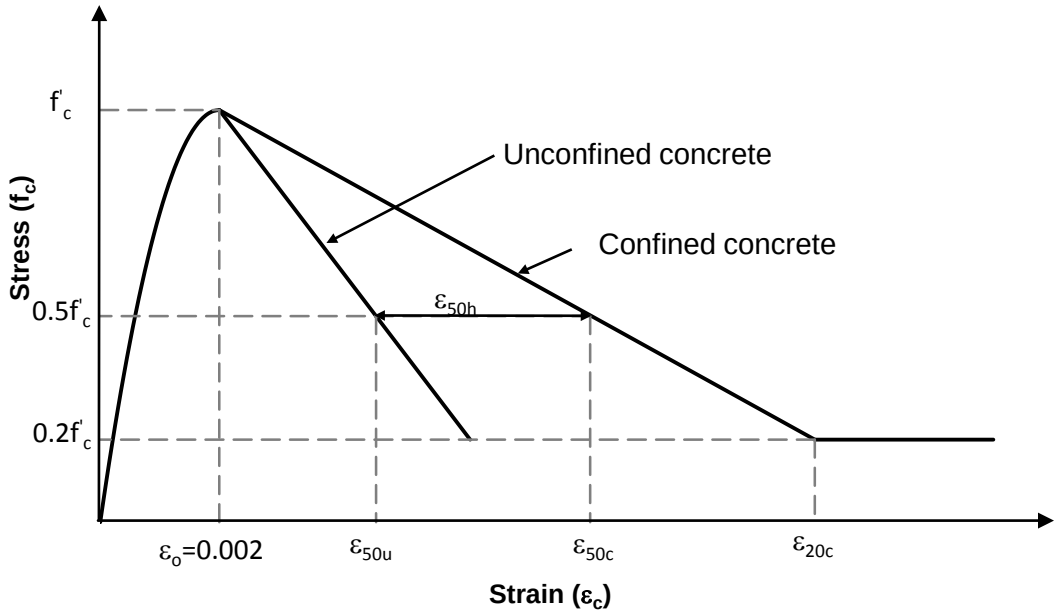

a. Proposed stress-strain model for confined and unconfined concrete – Kent and Park (1971) model.

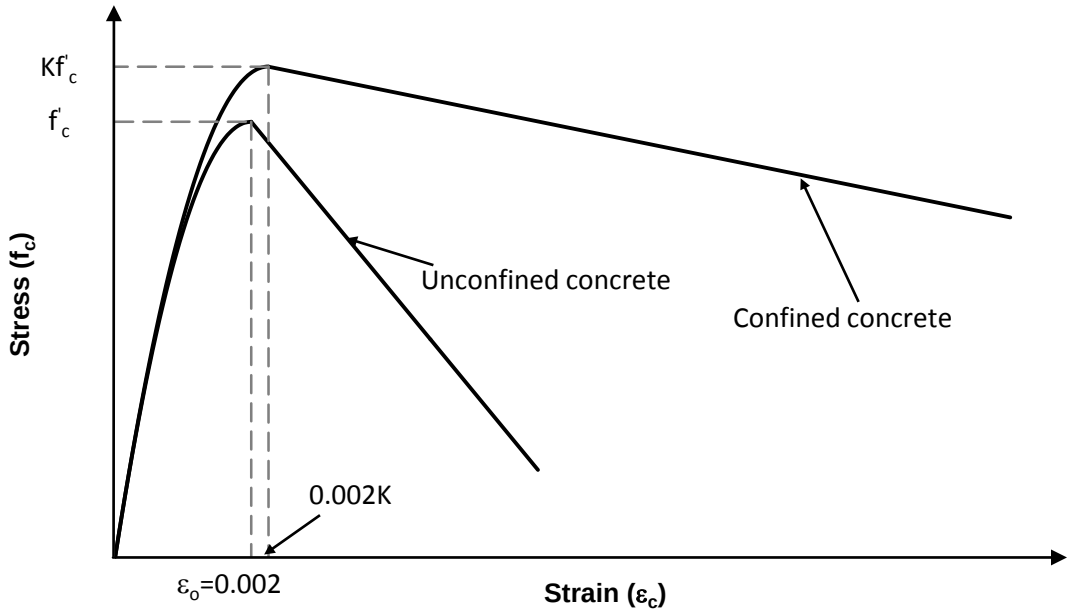

b. Stress-strain behavior of compressed concrete confined by rectangular steel hoops - Modified Kent and Park (Scott et al. 1982) model.

Figure 1: Stress-strain relationship for concrete proposed by earlier researchers.

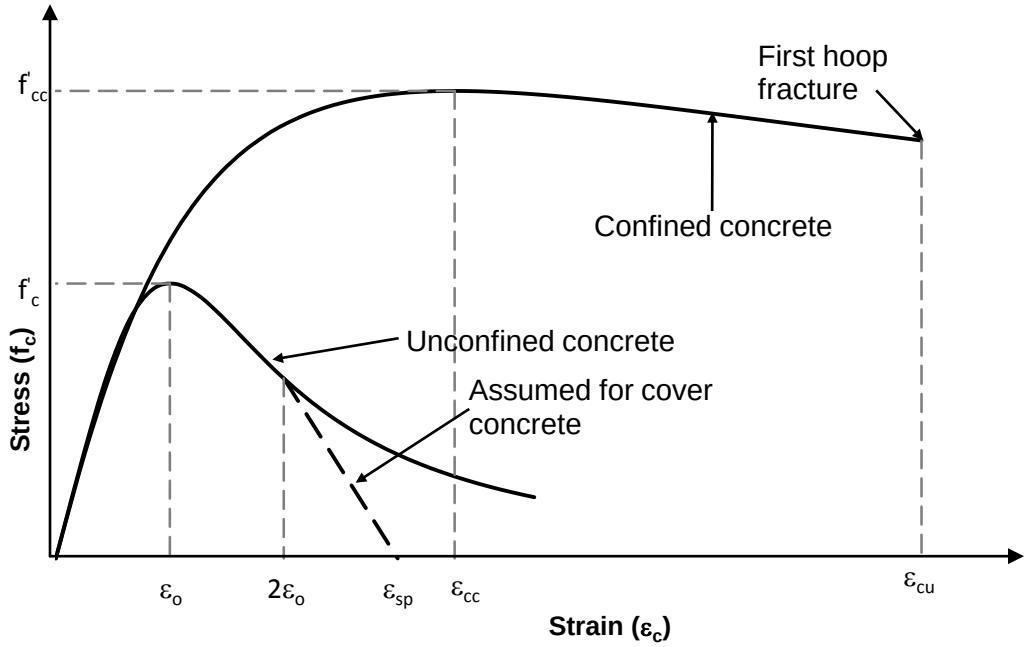

c. Stress-strain relation for monotonic loading of confined and unconfined concrete - Mander et al. (1988b).

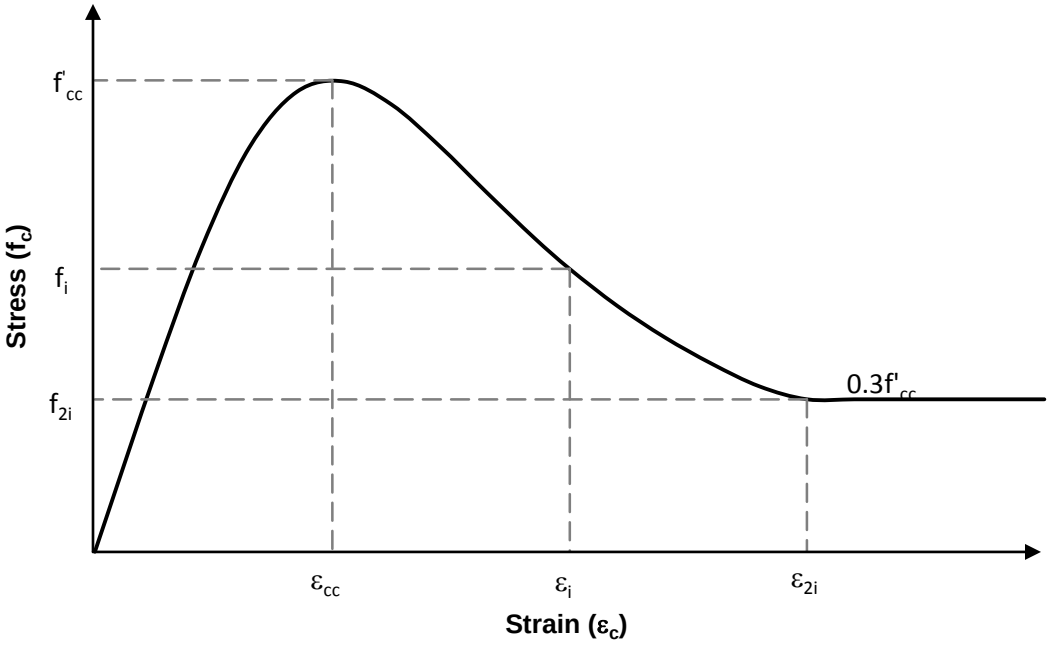

d. Stress-strain model for laterally confined high-strength concrete – Yong et al. (1989).

Figure 1 (continued)

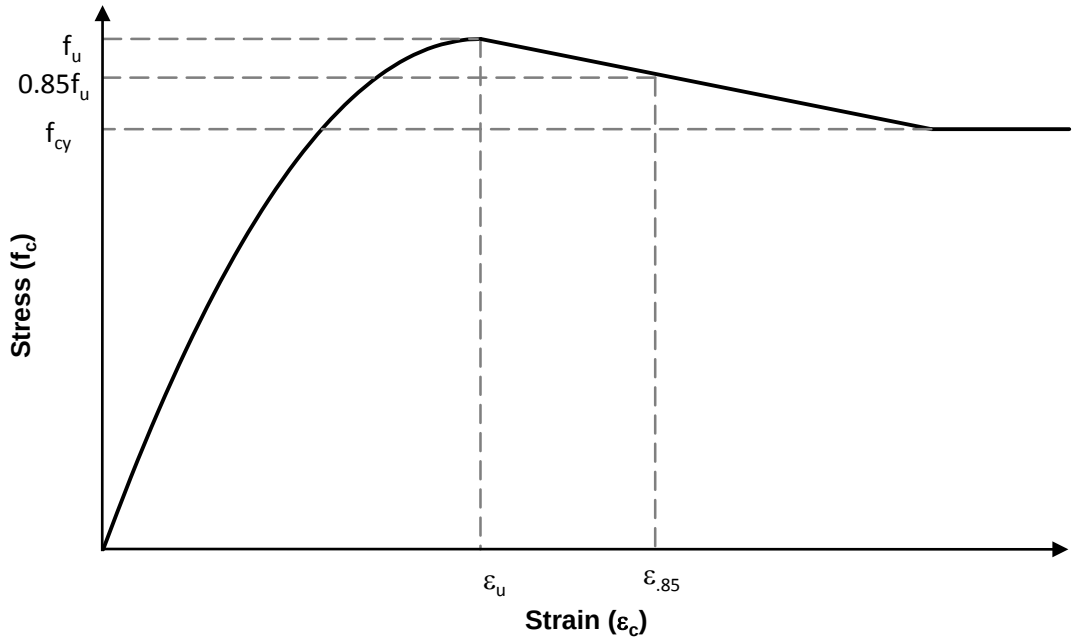

e. Theoretical stress-strain relation for confined concrete – Bjerkeli et al. (1990).

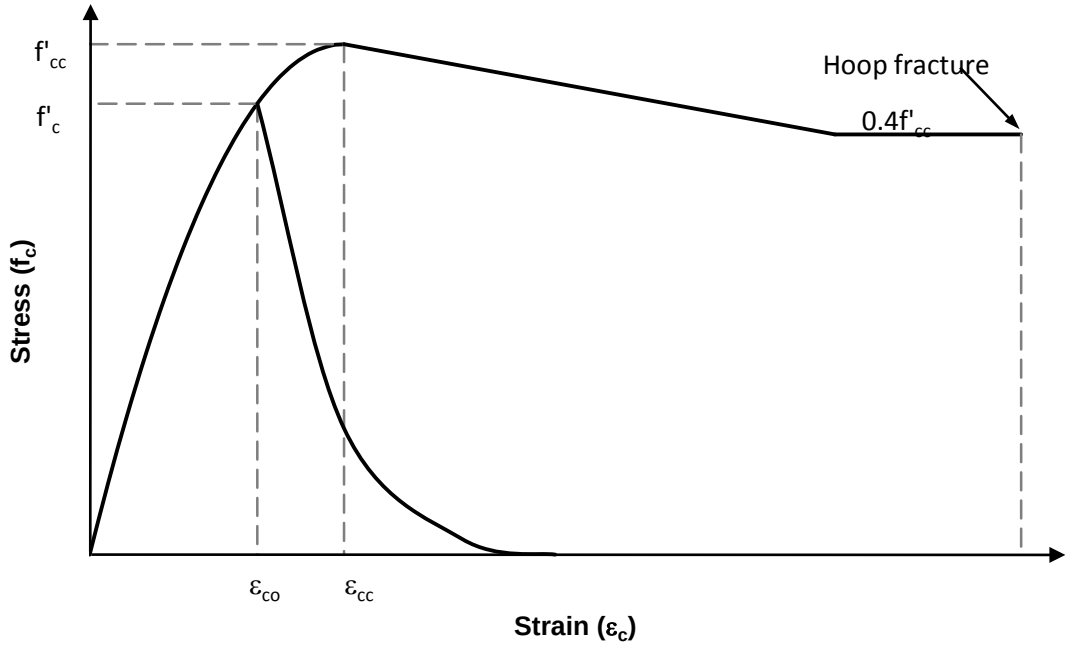

f. Stress-strain relation for confined high-strength concrete – Li et al. (2001).

Figure 1 (continued)

where $y = \frac{f_c}{f_c'}$ = ratio of the concrete stress to the ultimate strength, $x = \frac{\varepsilon}{\varepsilon_c}$ = ratio of concrete strain to the strain at $y = 1$, $m = \frac{E_o}{E_c}$ = ratio of initial tangent modulus to secant modulus at $y = 1$, $'n'$ = a factor to control the steepness rate of the descending portion of the stress-strain relation. The following expressions were defined for the factors $'m'$ and $'n'$.

$$m = 1 + \frac{17.9}{f_c'(MPa)}$$
$$m = 1 + \frac{2600}{f_c'(psi)} \quad (9)$$

$$n = \frac{f_c'}{6.68(MPa)} - 1.85 > 1$$
$$n = \frac{f_c'}{970(psi)} - 1.85 > 1 \quad (10)$$

Unfortunately, these additional parameters require considerable empirical calibration; moreover they lack any physical meaning and it is difficult to invert or integrate it in order to obtain the stress-block parameters.

CONFINED CONCRETE

Kent and Park (1971) made provisions in their stress-strain model to accommodate the behavior of confined concrete. Based on results from earlier tests on small square columns by Roy and Sozen (1964), it was shown that confining the concrete with rectangular or square hoops was not very effective and that there was either no substantial (or at best only a slight) increase in the concrete compressive strength due to confinement. For this reason it was assumed in this model that the

maximum stress reached by confined concrete remained the same as the unconfined cylinder strength, f_c'. Thus the ascending branch of the model is represented by the same second degree parabola.

Confinement only affected the slope of the post-peak branch and empirical equations were used to adjust this. The expression for the falling branch of the stress-strain relation is given by

$$f_c = f_c'[1 - Z(\varepsilon_c - \varepsilon_o)] \tag{11}$$

in which

$$Z = \frac{0.5}{\varepsilon_{50h+}\varepsilon_{50u} - \varepsilon_o} \tag{12}$$

where

$$\begin{aligned} \varepsilon_{50h} &= \varepsilon_{50c} - \varepsilon_{50u} \\ &= \frac{3}{4} p'' \sqrt{\frac{b''}{s}} \end{aligned} \tag{13}$$

where ε_{50c} and ε_{50u} are the strains corresponding to the stress equal to 50% of the maximum concrete strength for confined and unconfined concrete respectively.

$$\begin{aligned} \varepsilon_{50u} &= \frac{3 + 0.29 f_c'}{145 f_c' - 1000} \ (f_c' \ in \ MPa) \\ \varepsilon_{50u} &= \frac{3 + 0.002 f_c'}{f_c' - 1000} \ (f_c' \ in \ Psi) \end{aligned} \tag{14}$$

$\frac{b''}{s}$ is the ratio between the width of the concrete core and the center to center spacing of hoops, p'' is the volumetric ratio of confining hoops to volume of concrete core measured to the outside of the perimeter hoops and is expressed as

$$p'' = \frac{2(b'' + d'')A_s''}{b''d''s} \tag{15}$$

where b'' and d'' are the width and depth of the confined core respectively, A_s'' is the cross-sectional area of the hoop bar and $'s'$ is the center to center spacing of the hoops.

It is assumed that concrete can sustain some stress at indefinitely large strains. However, the failure of the member would occur before the strains in concrete become impractically high. Hence, for this model it was assumed that the concrete can sustain a stress of $0.2f_c'$ from a strain of ε_{20c} to infinite strain.

Desayi et al. (1978) based on tests conducted on circular columns with spiral lateral reinforcement proposed a single equation stress-strain model to represent the pre and post peak behavior of confined concrete and the equation was found to well represent the behavior of confined concrete.

$$f_c = \frac{A}{1 + B\varepsilon + C\varepsilon^2 + D\varepsilon^3} \tag{16}$$

where A, B, C and D were parameters that were obtained from boundary conditions and test results and are presented below.

$$A = E_c \tag{17}$$

$$B = \left[\frac{1 - 2k\beta + k\beta^2}{k(\beta - 1)^2}\frac{E_c}{E_c'} - \frac{2\beta + 1}{\beta}\right]\frac{1}{\varepsilon_{cc}} \quad (18)$$

$$C = \left[\frac{\beta + 2}{\beta} - \frac{2(1-k)}{k(\beta-1)^2}\frac{E_c}{E_c'}\right]\frac{1}{\varepsilon_{cc}^2} \quad (19)$$

$$D = \left[\frac{1-k}{k(\beta-1)^2}\frac{E_c}{E_c'} - \frac{1}{\beta}\right]\frac{1}{\varepsilon_{cc}^3} \quad (20)$$

in which

$$E_c' = \frac{f_{cc}'}{\varepsilon_{cc}} \quad (21)$$

$$\beta = \frac{\varepsilon_{0.85}}{\varepsilon_{cc}} = \frac{1.8 + 46.5C_i}{1.0 + 23.0C_i} \quad (22)$$

where 'k' is a constant = 0.85, C_i is the confinement index given by

$$C_i = (p_b - \bar{p}_b)\frac{f_y}{f_c'} \quad (23)$$

where p_b is the ratio of the volume of spiral to the volume of confined concrete, $\bar{p}_b$ is the value of p_b when the pitch of spiral is equal to the least lateral dimension of the specimen.

Scott et al. (1982) conducted experiments on a number of square concrete columns reinforced with either 8 or 12 longitudinal rebars and transversely reinforced with overlapping hoopsets. Their tests were conducted at rapid strain rates, typical of seismic loading. Unlike the Kent and Park (1971) model which was calibrated against small scale tests, they observed substantial strength enhancement due to the presence of good confining reinforcement details. Thus simple modifications were made to the Kent and Park (1971) model in order to incorporate the increase in the compressive strength of confined concrete at high strain rates (Figure 1b). The maximum concrete stress attained is assumed to be Kf_c' and the strain at maximum concrete stress is $0.002K$,

where 'K' is a factor that is defined later. The branches of the stress-strain curve for the modified Kent and Park relation for low strain rate is given as:

For $\varepsilon_c \leq 0.002\,K$ $$f_c = Kf_c'\left[\frac{2\varepsilon_c}{0.002K} - \left(\frac{\varepsilon_c}{0.002K}\right)^2\right] \quad (24)$$

For $\varepsilon_c > 0.002\,K$ $$f_c = Kf_c'[1 - Z_m(\varepsilon_c - 0.002K)] \quad (25)$$

But not less than $0.2Kf_c'$

in which

$$Z_m = \frac{0.5}{\frac{3 + 0.29f_c'}{145f_c' - 1000} + \frac{3}{4}\rho_s\sqrt{\frac{h''}{s_h}} - 0.002K} \quad (26)$$

where f_c' is in MPa, ρ_s = ratio of volume of rectangular steel hoops to volume of concrete core measured to the outside of the peripheral hoop, h''= width of concrete core measured to the outside of the peripheral hoop and s_h= center to center spacing of hoop sets. In the above expressions the value of $'K'$ is obtained from the following expression:

$$K = 1 + \frac{\rho_s f_{yh}}{f_c'} \quad (27)$$

where f_{yh} is the yield strength of the hoop reinforcement and rest of the parameters are as defined earlier.

For high strain rates the modified Kent and Park model can be used by using a multiplying factor of 1.25 to the peak stress, the strain at the peak stress and the slope of the falling branch. Thus, for high strain rates the expressions as presented in (24) and (25) can be used, but the values of 'K' and $'Z_m'$ are given as

$$K = 1.25\left[1 + \frac{p'' f_{yh}}{f_c'}\right] \tag{28}$$

$$Z_m = \frac{0.625}{\varepsilon_{50h} + \varepsilon_{50u} - 0.002K} \tag{29}$$

Mander et al. (1988a) first tested circular, rectangular and square full scale columns at seismic strain rates to investigate the influence of different transverse reinforcement arrangements on the confinement effectiveness and overall performance. Mander et al. (1988b) went on to model their experimental results. It was observed that if the peak strain and stress coordinates could be found ($\varepsilon_{cc}, f_{cc}'$), then the performance over the entire stress-strain range was similar, regardless of the arrangement of the confinement reinforcement used. Thus they adopted a failure criteria based on a 5-parameter model of William and Warnke (1975) along with data from Schickert and Winkler (1979) to generate a generalized multi-axial confinement model. Then to describe the entire stress-strain curve they adopted the 3-parameter equation proposed by Popovics (1973). The equations are represented as (Figure 1c):

$$\frac{f_c}{f_{cc}'} = \frac{n\left(\frac{\varepsilon_c}{\varepsilon_{cc}}\right)}{(n-1) + \left(\frac{\varepsilon_c}{\varepsilon_{cc}}\right)^n} \tag{30}$$

in which

$$n = \frac{E_c}{E_c - E_{sec}} \tag{31}$$

$$E_c(MPa) = 5000\sqrt{f_c'(MPa)} \tag{32}$$

$$E_{sec} = \frac{f_{cc}'}{\varepsilon_{cc}} \tag{33}$$

ε_{cc} is the strain at the maximum compressive strength of confined concrete f_{cc}'

$$\varepsilon_{cc} = \varepsilon_{co}\left[1 + 5\left(\frac{f'_{cc}}{f'_c} - 1\right)\right] \tag{34}$$

and f'_{cc}, the compressive strength of confined concrete is given as

$$f'_{cc} = f'_c\left(-1.254 + 2.254\sqrt{1 + \frac{7.94f'_l}{f'_c}} - 2\frac{f'_l}{f'_c}\right) \tag{35}$$

in which f'_l is given by

$$f_l' = \frac{1}{2}k_e\rho_s f_{yh} \tag{36}$$

in which ρ_s= ratio of volume of transverse confining steel to volume of confined concrete core, f_{yh}= yield strength of transverse reinforcement, k_e= confinement coefficient.

For circular hoops

$$k_e = \frac{\left(1 - \frac{s'}{2d_s}\right)^2}{1 - \rho_{cc}} \tag{37}$$

For circular spirals

$$k_e = \frac{1 - \frac{s'}{2d_s}}{1 - \rho_{cc}} \tag{38}$$

where ρ_{cc}= ratio of area of longitudinal reinforcement to area of core of the section, s'= clear spacing between spiral or hoop bars, d_s= diameter of spiral.

Due to its generality, the Mander et al. (1988b) model has enjoyed widespread use in design and research. Notwithstanding this it has several shortcomings. Since the original tests were developed in the 1980's, there has been a marked upsurge in the use of high performance (strength) materials, in particular high strength concrete. The

Mander et al. (1988b) model does not handle the post-peak branch of high strength concrete particularly well and requires some modification.

Yong et al. (1989) proposed stress-strain relation for rectilinear confined high-strength concrete. Their model consists of two polynomial equations which define the ascending and the post-peak branch (Figure 1d).

$$\varepsilon_c \leq \varepsilon_{cc} \qquad \frac{f_c}{f'_{cc}} = \frac{A\left(\frac{\varepsilon_c}{\varepsilon_{cc}}\right) + B\left(\frac{\varepsilon_c}{\varepsilon_{cc}}\right)^2}{1 + (A-2)\left(\frac{\varepsilon_c}{\varepsilon_{cc}}\right) + (B+1)\left(\frac{\varepsilon_c}{\varepsilon_{cc}}\right)^2} \tag{39}$$

$$\varepsilon_c \geq \varepsilon_{cc} \qquad \frac{f_c}{f'_{cc}} = \frac{C\left(\frac{\varepsilon_c}{\varepsilon_{cc}}\right) + D\left(\frac{\varepsilon_c}{\varepsilon_{cc}}\right)^2}{1 + (C-2)\left(\frac{\varepsilon_c}{\varepsilon_{cc}}\right) + (D+1)\left(\frac{\varepsilon_c}{\varepsilon_{cc}}\right)^2} \tag{40}$$

in which the parameters A through D are as defined below.

$$A = E_c \frac{\varepsilon_{cc}}{f'_{cc}} \tag{41}$$

$$B = \frac{(A-1)^2}{0.55} - 1 \tag{42}$$

where

$$E_c = 27.55 w^{1.5} \sqrt{f'_c} \tag{43}$$

$$C = \frac{(\varepsilon_{2i} - \varepsilon_i)}{\varepsilon_{co}} \left[\frac{\varepsilon_{2i} E_i}{f'_{cc} - f_i} - \frac{4\varepsilon_i E_{2i}}{f'_{cc} - f_{2i}}\right] \tag{44}$$

$$D = (\varepsilon_i - \varepsilon_{2i}) \left[\frac{E_i}{f'_{cc} - f_i} - \frac{4E_{2i}}{f'_{cc} - f_{2i}}\right] \tag{45}$$

$$E_i = \frac{f_i}{\varepsilon_i} \; and \; E_{2i} = \frac{f_{2i}}{\varepsilon_{2i}} \tag{46}$$

The other parameters are defined below.

$$f'_{cc} = kf'_c = 1 + 0.0091\left(1 - \frac{0.245s}{h''}\right)\left(\rho'' + \frac{nd''}{8sd}\rho\right)\frac{f''_y}{\sqrt{f'_c}} \quad (47)$$

$$\varepsilon_{co} = 0.00265 + \frac{0.0035\left(1 - \frac{0.734s}{h''}\right)\left(\rho'' f''_y\right)^{2/3}}{\sqrt{f'_c}} \quad (48)$$

$$f_i = f'_{cc}\left[0.25\left(\frac{f'_c}{f'_{cc}}\right) + 0.4\right] \quad (49)$$

$$\varepsilon_i = K\left[1.4\left(\frac{\varepsilon_o}{K}\right) + 0.003\right] \quad (50)$$

$$f_{2i} = f'_{cc}\left[0.025\left(\frac{f'_{cc}}{1000}\right) - 0.065\right] \geq 0.3f'_{cc} \quad (51)$$

$$\varepsilon_{2i} = 2\varepsilon_i - \varepsilon_{co} \quad (52)$$

Bjerkeli et al. (1990) conducted a series of experiments in order to study the ductility of confined axially loaded high strength concrete reinforced columns. From the test results and a review of earlier work the authors identified that concrete compressive strength, confining reinforcement ratio and section geometry as the major parameters that control the stress-strain relation of confined concrete.

The authors identified that a convenient way of expressing the confining reinforcement ratio is by using the idealized "confining pressure", f_r, which is defined as

$$f_r = \frac{A_{sh} f_{sy}}{h' s_p} \quad (53)$$

where h' = outer size of the confined section, A_{sh} = total effective area of hoop ties and supplementary confining reinforcement in direction under consideration within spacing

s_p, f_{sy} = yield stress of confining reinforcement, s_p = center distance between hoop/ties confining reinforcement.

The influence of the section geometry was represented by the "section geometry factor", K_g, which expresses the effective concrete core cross-section after compression arches have developed. The section geometry factor associated with the development of compression arches in the vertical direction between the confinement reinforcement layers is expressed as (Shah et al. (1983)):

$$K_{g1} = 1 - \frac{s_p}{d_{so}} \tag{54}$$

where d_{so}= the shorter outer diameter of hoop ties and s_p is as defined earlier.

Another factor, calculated for compression arches between laterally supported longitudinal reinforcement is expressed as (Sheikh at al. (1986)):

$$K_{g2} = 1 - \frac{nC^2}{5.5A_c'} \tag{55}$$

where n = number of laterally supported longitudinal bars, C = distance between the laterally supported longitudinal bars, A_c'= gross area of concrete section measured to center line of peripheral hoop. The larger of the two values K_{g1} and K_{g2} is taken as the value of K_g in the proposed stress strain model.

The equations for the confined concrete stress-strain model proposed by Bjerkeli et al. (1990) are presented below and shown in Figure 1e.

i. Ascending branch

$$\varepsilon \leq \varepsilon_u \qquad \sigma = \frac{E_c \varepsilon}{1 + \left(\frac{E_c}{E_o} - 2\right)\left(\frac{\varepsilon}{\varepsilon_u}\right) + \left(\frac{\varepsilon}{\varepsilon_u}\right)^2} \tag{56}$$

ii. Descending branch

$$\varepsilon > \varepsilon_u \qquad \sigma = f_u - Z(\varepsilon - \varepsilon_u) \tag{57}$$

iii. Horizontal part

$$\sigma = f_{cy} = 4.87 \frac{d_{sp} A_{sh} f_{sy}}{s_p A_c} \tag{58}$$

where

$$Z = \frac{0.15\, f_u}{\varepsilon_{.85} - f_u} \tag{59}$$

$$E_o = \frac{f_u}{\varepsilon_u} \tag{60}$$

$$E_c = 9500 \left(\frac{\rho_c}{2400}\right)^{1.5} {f_c'}^{0.3} \tag{61}$$

For normal density concrete

$$\begin{aligned} 45\ MPa < f_c' \leq 80\ MPa \qquad & f_u = f_c + 4\ K_g f_r \\ 80\ MPa < f_c' < 90\ MPa \qquad & f_u = f_c + 3\ K_g f_r \end{aligned} \tag{62}$$

$$\varepsilon_u = 0.0025 + 0.05 K_g \left(\frac{f_r}{f_c'}\right) \tag{63}$$

$$\varepsilon_{.85} = \varepsilon'_{.85} + \frac{0.05 K_g \left(\frac{f_r}{f_c'}\right)}{1 - F} \tag{64}$$

$$\varepsilon'_{.85} = 0.0025 \left[\left(\frac{17.07}{f_c'}\right)^2 + 1\right] \tag{65}$$

For light weight aggregate concrete

$45\ MPa < f_c' < 70\ MPa$

$$f_u = f_c + 1.5\ K_g f_r \tag{66}$$

$$\varepsilon_u = 0.0030 + 0.025 K_g \left(\frac{f_r}{f_c'}\right) \tag{67}$$

$$\varepsilon_{.85} = \varepsilon'_{.85} + \frac{0.025 K_g \left(\frac{f_r}{f_c'}\right)}{1 - F} \tag{68}$$

$$\varepsilon'_{.85} = 0.0030 \left[\left(\frac{12.41}{f_c'}\right)^2 + 1\right] \tag{69}$$

The term $'F'$ for both normal density and light weight aggregate concrete is expressed as

$$F = \frac{1}{1 + \left(\frac{1}{f_r K_g}\right)^{0.25}} \tag{70}$$

where K_g and f_r are as defined earlier.

Again as in the case of earlier models, the equations are complex and cannot be easily inverted or integrated in order to obtain the equivalent rectangular stress-block parameters.

Li et al. (2000) conducted an experimental investigation on circular and square reinforced concrete columns to study the behavior of high-strength concrete columns confined by normal and high-yield strength transverse reinforcement and with different confinement ratio and configurations. From the tests they concluded that volumetric ratio and the yield strength of confining reinforcement significantly affect the shape of the stress-strain curve. Based on their experimental study, Li et al. (2001) proposed a three branch stress-strain model for high strength concrete confined by either normal or high-yield strength transverse reinforcement (Figure 1f). The equations are:

$$0 < \varepsilon_c \leq \varepsilon_{co} \qquad f_c = E_c\varepsilon_c + \frac{(f_c' - E_c\varepsilon_{co})}{\varepsilon_{co}^2}\varepsilon_c^2 \tag{71}$$

$$\varepsilon_{co} < \varepsilon_c \leq \varepsilon_{cc} \qquad f_c = f_{cc}' - \frac{(f_{cc}' - f_c')}{(\varepsilon_{cc} - \varepsilon_{co})^2}(\varepsilon_c - \varepsilon_{cc})^2 \tag{72}$$

$$\varepsilon_c > \varepsilon_{cc} \qquad f_c = f_{cc}' - \beta\frac{f_{cc}'}{\varepsilon_{cc}}(\varepsilon_c - \varepsilon_{cc}) \geq 0.4f_{cc}' \tag{73}$$

The term β controls the slope of the post-peak branch of the stress-strain model. The maximum confined concrete compressive strength is given by

$$f_{cc}' = f_c'\left(-1.254 + 2.254\sqrt{1 + \frac{7.94f_l'}{f_c'}} - 2\alpha_s\frac{f_l'}{f_c'}\right) \tag{74}$$

in which

$$\text{when } f_c' \leq 52\ MPa \qquad \alpha_s = (21.2 - 0.35f_c')\frac{f_l'}{f_c'} \tag{75}$$

$$\text{when } f_c' > 52\ MPa \qquad \alpha_s = 3.1\frac{f_l'}{f_c'} \tag{76}$$

where f_l' is the effective lateral confining pressure, calculated using the equations proposed by Mander et al. (1988b) as in (36) to (38).

The expressions for axial strain at maximum strength (ε_{cc}), factor to control the slope of the descending branch β and maximum concrete strain ε_{cu}; for circular and rectilinear confinement using normal-strength and high-strength steel can be found in the author's paper.

1.5 Stress-Block Analysis

Stress-blocks have been used in design based on the early work of Whitney (1942). But these are normally for a specific maximum strain. For example ACI 318 customarily uses $\varepsilon_c = 0.003$ to define the nominal strength. However, as pointed out in Park and Pauley (1975), stress-blocks may be used across a spectrum of maximum strains. Indeed a stress-block approach could be used to analytically generate an entire moment-curvature response.

Hognestad (1951) expressed the compression force in the concrete as $C = k_1 bcf_c'$ and the distance to the centroid of the stress-block from the extreme compression fiber as $k_2 c$, where 'c' is the depth to the neutral axis, 'b' is the breadth of the section and k_1 and k_2 factors that were determined (Table 1).

Kent and Park (1971) based on their stress-strain relation of unconfined and confined concrete gave values of mean stress factor (α) and the centroid factor (γ) for extreme fiber concrete compression strains greater than 0.002 for different values of the post-peak branch slope 'Z' (Table 2).

Table 1: Stress-block parameters proposed by Hognestad (1951).

$f_c'\ (Psi)$	k_1	k_2
0	0.925	0.513
1000	0.873	0.481
2000	0.835	0.459
3000	0.808	0.444
4000	0.786	0.432
5000	0.770	0.423
6000	0.758	0.417

Table 2: Stress-block parameters α and γ as a function of ε_{cm} and Z – Kent and Park (1971).

	Z								
ε_{cm}	10	30	50	70	100	140	200	300	400
Values of α									
0.002	0.667	0.667	0.667	0.667	0.667	0.667	0.667	0.667	0.667
0.003	0.776	0.773	0.769	0.766	0.761	0.754	0.744	0.728	0.711
0.004	0.828	0.818	0.808	0.798	0.783	0.763	0.733	0.683	0.633
0.005	0.858	0.840	0.822	0.804	0.777	0.741	0.687	0.600	0.547
0.006	0.876	0.849	0.822	0.796	0.756	0.702	0.622	0.533	0.489
0.007	0.887	0.851	0.815	0.780	0.726	0.655	0.562	0.486	0.448
0.008	0.894	0.849	0.804	0.759	0.692	0.602	0.517	0.450	0.417
0.009	0.899	0.844	0.790	0.735	0.654	0.558	0.481	0.422	0.393
0.010	0.901	0.837	0.773	0.709	0.613	0.522	0.453	0.400	0.373
0.011	0.903	0.829	0.755	0.682	0.576	0.493	0.430	0.382	0.358
0.012	0.903	0.819	0.736	0.653	0.544	0.468	0.411	0.367	0.344
0.013	0.902	0.809	0.716	0.623	0.518	0.448	0.395	0.354	0.333
0.014	0.901	0.798	0.695	0.593	0.495	0.430	0.381	0.343	0.324
0.015	0.899	0.787	0.674	0.567	0.476	0.415	0.369	0.333	0.316
Values of γ									
0.002	0.375	0.375	0.375	0.375	0.375	0.375	0.375	0.375	0.375
0.003	0.405	0.407	0.408	0.409	0.411	0.414	0.418	0.425	0.432
0.004	0.427	0.430	0.433	0.436	0.441	0.449	0.460	0.482	0.507
0.005	0.441	0.446	0.452	0.457	0.466	0.479	0.501	0.543	0.568
0.006	0.451	0.459	0.466	0.474	0.488	0.508	0.545	0.586	0.602
0.007	0.459	0.469	0.479	0.490	0.508	0.538	0.582	0.611	0.622
0.008	0.466	0.477	0.490	0.504	0.529	0.570	0.607	0.627	0.633
0.009	0.471	0.484	0.500	0.518	0.550	0.595	0.623	0.636	0.638
0.010	0.475	0.491	0.509	0.531	0.573	0.613	0.634	0.641	0.641
0.011	0.479	0.497	0.519	0.546	0.594	0.626	0.641	0.644	0.642
0.012	0.482	0.503	0.528	0.560	0.610	0.635	0.645	0.645	0.641
0.013	0.485	0.508	0.538	0.576	0.622	0.642	0.648	0.645	0.640
0.014	0.488	0.514	0.547	0.592	0.631	0.646	0.649	0.644	0.638
0.015	0.490	0.519	0.557	0.606	0.638	0.650	0.649	0.642	0.635

Mander (1983) based on his stress-strain relation for confined concrete proposed the stress-block parameters (α and β) for different levels of confinement. The results of the stress-block parameters for different levels of confinement are presented in Figure 2.

Azizinamini et al. (1994) conducted tests on high-strength concrete columns and observed that the maximum measured moment for test columns with concrete compressive strengths exceeding 97 MPa were less than the moment determined using the stress-block parameters recommended by ACI 318-89. The authors proposed an alternate procedure to conservatively predict the nominal moment capacities of columns with f_c' > 97 MPa. It was considered appropriate to use triangular stress-blocks for calculating the flexural capacity of columns with compressive strength exceeding 69 MPa. The maximum compressive strength was assumed to be $0.85f_c'$ at an axial compressive strain of 0.003. The equivalent rectangular stress-blocks were found to have the compressive stress intensity as $0.63f_c'$ in place of $0.85f_c'$ as recommended by ACI 318-89 and the depth of the rectangular stress-block was found to be 0.67 times the depth to the neutral axis. Based on these findings the authors proposed that for concrete compressive strengths greater than 69 MPa the stress intensity factor of the equivalent rectangular stress-block must be reduced from 0.85 using the following expression

$$Stress\ intensity = 0.85 - 0.05\left(\frac{f_c' - 10000}{10000}\right) \geq 0.60 \qquad (77)$$

Ibrahim and MacGregor (1997) proposed equations for the stress-block parameters α and β. The equation proposed for β was found to pass through the center

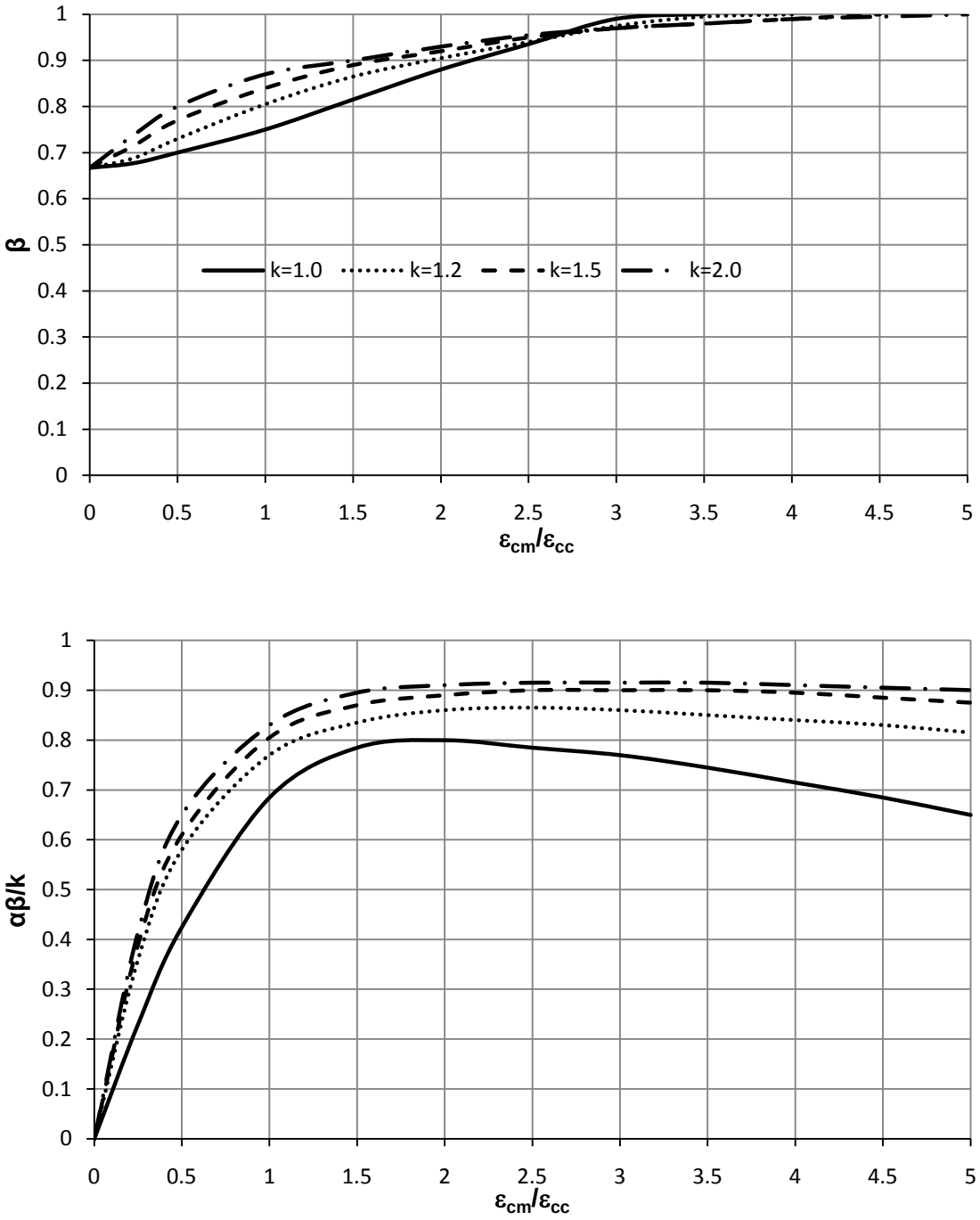

Figure 2: Equivalent rectangular stress-block parameters for rectangular sections with confined concrete – Mander (1983).

of the experimental data points and was conservative compared to the ACI 318-89 equation for different concrete strengths. The expression for β is as represented below.

$$\beta = 0.95 - \frac{f_c'}{400} \geq 0.70 \quad (78)$$

The authors also observed that a constant value of $\alpha = 0.85$ would provide a safe design for high strength and ultra high strength concrete sections and would give very conservative design for normal strength concrete sections. The authors proposed an equation for α that decreased with increase in the concrete compressive strength.

$$\alpha = 0.85 - \frac{f_c'}{800} \geq 0.725 \quad (79)$$

For concrete strength greater than 100 MPa constant values of $\alpha = 0.725$ and $\beta = 0.70$ were adopted.

Attard and Steward (1998) noted that the ACI 318-95 formula for the stress-block parameter are limited to concrete with concrete compressive strength of up to 50 MPa. In the ACI 318-95 stress-blocks parameter, the stress-block depth parameter is varied with the concrete strength and the width of the equivalent rectangular stress-block is defined as a constant value 0.85 times the compressive strength of concrete.

However, the authors propose that to extend the stress-block parameters to high-strength concrete, a two-parameter model is necessary. The equivalent rectangular stress-block parameters are defined by the parameter $k_1 k_3$ (equivalent to α) and k_2 (equivalent to β). k_1 defines the width of the equivalent stress-block, k_2 defines the stress-block depth factor and the factor k_3 takes into the account the factors that

contribute to the differences between the in-situ compressive strength and the strength determined from standard cylinder compression tests. The expressions for these factors are given below.

Mean from dogbone (DB) tests

$$k_3 = 1.05 - 0.0009 f_{cyl} \tag{80}$$

Mean inc. sustained load (SL) effects

$$k_3 = \phi_{SL}\left(1.05 - 0.0009 f_{cyl}\right) \tag{81}$$

in which the sustained load factor is given by

$$\phi_{SL} = (0.71 + 0.002 f_{cyl}) \leq 1 \tag{82}$$

where f_{cyl} is the mean cylinder compressive concrete strength given by

$$f_{cyl} \cong f_c' + 7.5\ MPa \tag{83}$$

$$\begin{aligned} k_1 k_3 &= 1.2932 {f_c'}^{-0.0998} \geq 0.71 \quad Mean\ (k_3 DB) \\ &= 1.4037 {f_{cyl}}^{-0.116} \geq 0.71 \end{aligned} \tag{84}$$

$$\begin{aligned} k_1 k_3 &= 0.6470 {f_c'}^{0.0324} \geq 0.58 \quad Mean\ (k_3 SL) \\ &= 0.6292 {f_{cyl}}^{0.0379} \geq 0.58 \end{aligned} \tag{85}$$

$$\begin{aligned} k_2 &= 1.0948 {f_c'}^{-0.091} \geq 0.67 \\ &= 1.0276 {f_{cyl}}^{-0.0785} \geq 0.67 \end{aligned} \tag{86}$$

In the next section a stress-strain model for unconfined and confined concrete applicable to both normal and high-strength concrete is proposed and closed form equations for the stress-block parameters are derived.

2. PROPOSED STRESS-STRAIN MODEL FOR UNCONFINED AND CONFINED CONCRETE

2.1 Introduction

The proposed stress-strain model of both unconfined and confined concrete in compression is set by three coordinates as depicted in Figure 3. For unconfined concrete these are: the peak strength (ε_{co}, f_c'), at the termination of the post-peak branch $(\varepsilon_{c1}, f_{c1})$, and the failure strain $(\varepsilon_{sp}, 0)$. Similarly, for confined concrete the principal control coordinates are: $(\varepsilon_{cc}, f_{cc}'), (\varepsilon_{cu}, f_{cu})$ and $(\varepsilon_f, 0)$. Using these coordinates as commencement and termination points, the proposed stress-strain model has three branches – an initial power curve up to the peak stress, followed by a bilinear relation in the post-peak region. The expressions representing the proposed stress-strain relation are presented below.

$$0 \le x < 1 \qquad f_c = Kf_c'(1 - |1 - x|^n) \tag{87}$$

$$1 \le x < x_u \qquad f_c = Kf_c' - (f_c' - 12)\left(\frac{x - 1}{x_u - 1}\right) \tag{88}$$

$$x_u \le x < x_f \qquad f_c = f_{cu}\left(\frac{x - x_f}{x_u - x_f}\right) \tag{89}$$

in which K = confinement ratio and for confined concrete ($K > 1$); $x = \frac{\varepsilon_c}{\varepsilon_{cc}}$, $x_u = \frac{\varepsilon_{cu}}{\varepsilon_{cc}} = 5$ and $x_f = \frac{\varepsilon_f}{\varepsilon_{cc}}$. The various parameters in the above equations are defined below.

$$\varepsilon_{cc} = \varepsilon_{co}\big(1 + 5(K - 1)\big) \tag{90}$$

$$\varepsilon_{co} = 0.0015 + \frac{f_c'\ (MPa)}{70000} \tag{91}$$

$$E_c = \ 5000\sqrt{f_c'(MPa)} \tag{92}$$

For unconfined concrete

$$n = \frac{E_c\ \varepsilon_{co}}{f_c'} \tag{93}$$

For confined concrete

$$n = \frac{E_c \varepsilon_{cc}}{f_{cc}'} \tag{94}$$

$$\varepsilon_{sp} = 0.012 - 0.0001 f_c' \tag{95}$$

$$f_{cu} = 12 + f_c'(K-1)\ in\ MPa \tag{96}$$

The expression for f_{cu} was obtained from experimental results of Mander et al. (1988a) and Li et al. (2000). The scatter of the experimental values of f_{cu} and the straight line fit (96) are presented in Figure 4.

Compared to other stress-strain models, (e.g. Popovics, 1973), an advantage of the above three equations is that they can be easily inverted to find the strain explicitly as a function of stress as follows.

$$x = \left[1 - \left(1 - \frac{f_c}{K f_c'}\right)^{\frac{1}{n}}\right] \tag{97}$$

$$x = \left[1 + \left(\frac{K f_c' - f_c}{f_c' - 12}\right)(x_u - 1)\right] \tag{98}$$

$$x = x_f + \frac{f_c}{f_{cu}}\left(x_u - x_f\right) \tag{99}$$

For unconfined concrete $(K = 1)$, $\varepsilon_{cc} = \varepsilon_{co}, \varepsilon_{cu} = \varepsilon_{c1}\ (= 0.0036), \varepsilon_f = \varepsilon_{sp}$ and $f_{cu} = f_{c1}$ in all of the above equations. The stress-strain plot for unconfined and

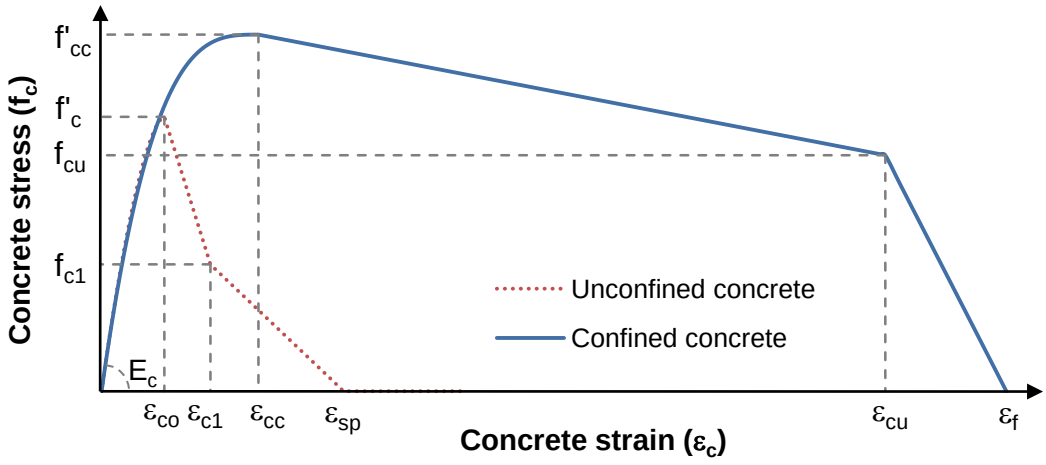

Figure 3: Proposed stress-strain model for unconfined and confined concrete.

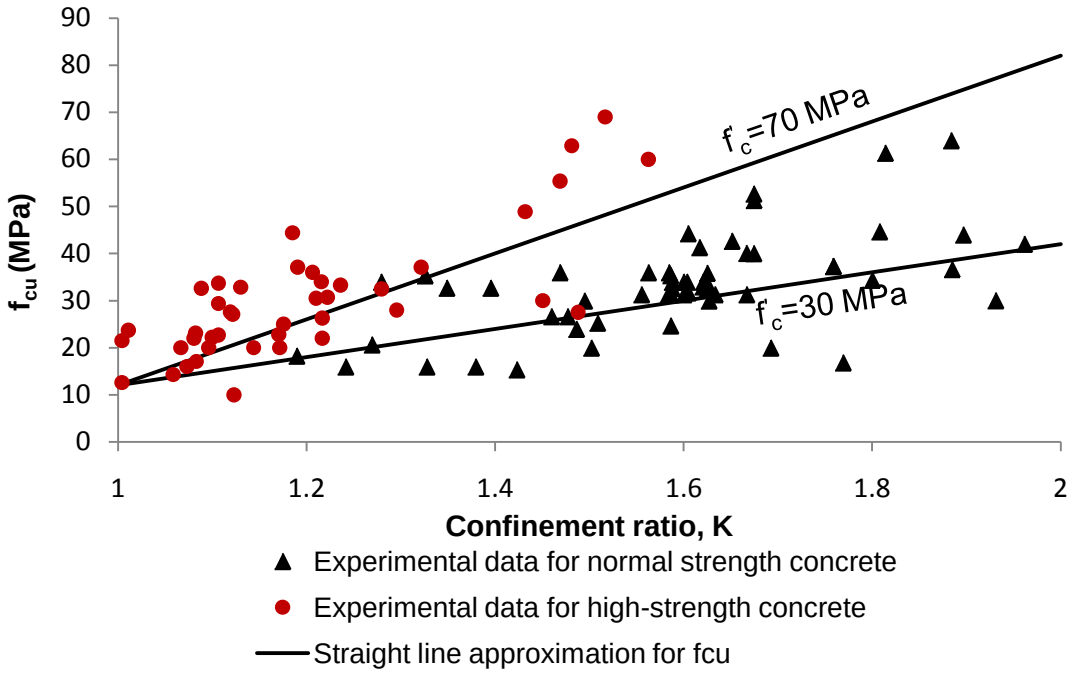

Figure 4: Calibration of f_{cu} from experimental data.

confined concrete of different compressive strengths is plotted in the figures shown in Appendix I and II.

2.2 Stress-Strain Model for Unconfined Concrete in Tension

For the stress-strain model of unconfined concrete in tension, the same model as described above for unconfined concrete in compression can be used. However, the parameters need to be defined for the tensile behavior of concrete. Measured values may be used, or as a good approximation the values of f_t', ε_{to}, f_{tc1}, ε_{tc1} and ε_{tsp} can be taken as one-tenth of their corresponding values in compression.

2.3 Equivalent Rectangular Stress-Block Parameters

Equivalent rectangular stress-block parameters are extensively used in the analysis and design of concrete structural members and offer a convenient way to determine flexural capacity. These parameters are derived from the stress-strain relation of concrete. In order to determine the stress-block parameters, the effective average concrete stress ratio (α) and the effective stress-block depth factor (β), the area and the first moment of area under the stress-strain curve of concrete and the effective rectangular stress-block are equated. One of the major advantages of the proposed stress-strain model is that, they can be easily integrated and closed form equations can be established for the stress-block parameters. The procedure to obtain the stress-block parameters follows.

The force in concrete (C_c) for a known value of strain can be expressed in terms of equivalent stress-block parameters α and β such that:

$$C_c = \alpha f_c' \beta c b \tag{100}$$

where c = depth to the neutral axis from the top concrete fiber in compression; and b = breadth of the section.

The area and the first moment of area of the stress-strain function are given by

$$A_c = \int_0^{\varepsilon_c} f_c \, d\varepsilon_c = \alpha f_c' \beta \varepsilon_c \tag{101}$$

$$A\bar{y} = \int_0^{\varepsilon_c} f_c \varepsilon_c d\varepsilon_c = \left(1 - \frac{\beta}{2}\right) \varepsilon_c \int_0^{\varepsilon_c} f_c \, d\varepsilon_c \tag{102}$$

from which the stress-block parameters can be found from

$$\alpha\beta = \frac{\int_0^{\varepsilon_c} f_c \, d\varepsilon_c}{f_c' \varepsilon_c} \tag{103}$$

and

$$\beta = 2 - 2\frac{\int_0^{\varepsilon_c} f_c \varepsilon_c d\varepsilon_c}{\varepsilon_c \int_0^{\varepsilon_c} f_c d\varepsilon_c} \tag{104}$$

Carrying out the integration in (103) and (104) using the stress-strain relations (87) to (89) gives the stress block relations as follows:

i. For $0 \leq x < 1$

$$\alpha\beta = 1 + \frac{(1-x)^{n+1} - 1}{x(n+1)} \tag{105}$$

$$\beta = 2 - \frac{2}{x^2 \alpha\beta}\left[\frac{x^2}{2} + \frac{x(1-x)^{n+1}}{(n+1)} + \frac{(1-x)^{n+2} - 1}{(n+1)(n+2)}\right] \tag{106}$$

ii. For $1 \leq x < x_{cu}$

$$\alpha\beta = \frac{A_1}{x} - \frac{x-1}{x(x_u - 1)}\left[A_2 - x_u + x\frac{(f_c' - 12)}{2Kf_c'}\right] \tag{107}$$

$$\beta = 2 - \frac{1}{x^2\alpha\beta}\left[B_1 + (x^2 - 1) - \left(\frac{f_c' - 12}{3Kf_c'}\right)\left(\frac{2x^3 - 3x^2 + 1}{x_u - 1}\right)\right] \quad (108)$$

iii. For $x_u \leq x < x_f$

$$\alpha\beta = \frac{A_1}{x} + A_2\left(\frac{x_u - 1}{x}\right) + \frac{f_{cu}}{2Kf_c'}\frac{(x - x_u)(x + x_u - 2x_f)}{x(x_u - x_f)} \quad (109)$$

$$\beta = 2 - \frac{1}{x^2\alpha\beta}\left[B_1 + B_2 + B_3 + \frac{f_{cu}}{3Kf_c'}\left(\frac{3x_f{x_u}^2 - 2{x_u}^3 + x^2(2x - 3x_f)}{x_u - x_f}\right)\right] \quad (110)$$

iv. For $x \geq x_f$

$$\alpha\beta = \frac{A_1}{x} + A_2\left(\frac{x_u - 1}{x}\right) + \frac{f_{cu}}{2Kf_c'}\left(\frac{x_f - x_u}{x}\right) \quad (111)$$

$$\beta = 2 - \frac{B_1 + B_2 + B_3 + B_4}{x^2\alpha\beta} \quad (112)$$

In the above the following coefficients are used

$$A_1 = \frac{n}{(n+1)} \quad (113)$$

$$A_2 = \left(\frac{12 + f_c'(2K - 1)}{2Kf_c'}\right) \quad (114)$$

$$B_1 = \frac{n(n+3)}{(n+1)(n+2)} \quad (115)$$

$$B_2 = ({x_u}^2 - 1) \quad (116)$$

$$B_3 = \frac{(12 - f_c')}{3Kf_c'}\left(\frac{2{x_u}^3 - 3{x_u}^2 + 1}{x_u - 1}\right) \quad (117)$$

$$B_4 = \frac{f_{cu}}{3Kf_c'}\left(\frac{3x_f{x_u}^2 - 2{x_u}^3 - {x_f}^3}{x_u - x_f}\right) \quad (118)$$

In the above expressions $x = \frac{\varepsilon_c}{\varepsilon_{cc}}, x_u = \frac{\varepsilon_{cu}}{\varepsilon_{cc}}$ and $x_f = \frac{\varepsilon_f}{\varepsilon_{cc}}$. For unconfined concrete $K = 1,\ \varepsilon_{cc} = \varepsilon_{co}, \varepsilon_{cu} = \varepsilon_{c1}, \varepsilon_f = \varepsilon_{sp}\ and\ f_{cu} = f_{c1}$. The stress-block parameters are shown in Figure 5.

2.4 Worked Example Using Stress-Blocks

COMPUTATIONAL SOLUTION IMPLEMENTATION

The computational solution is implemented to perform an analytical moment-curvature analysis in two ways. First, the derived stress-block parameters are used and in the second a fiber analysis using the proposed stress-strain relation is carried out. In the latter solution procedure, the concrete section is divided into a number of fibers and the strains (and hence the stresses) are calculated at their centers knowing the centroidal strain ε_o, curvature ϕ and the distance to the center of the layer from the centroidal axis y. A general procedure of determining the moment-curvature relation for columns under axial load is outlined in the following steps.

Step 1: To the value of the last known curvature solution ϕ_{k-1}, the curvature increment $\Delta\phi$ is added to give the new curvature,

$$\phi_k = \phi_{k-1} + \Delta\phi \tag{119}$$

Step 2: For an incremental curvature ($\Delta\phi$) and an associated augment in the reference axis strain ($\Delta\varepsilon_o$), the change in axial force (ΔP) and moment (ΔM) over that step is found by

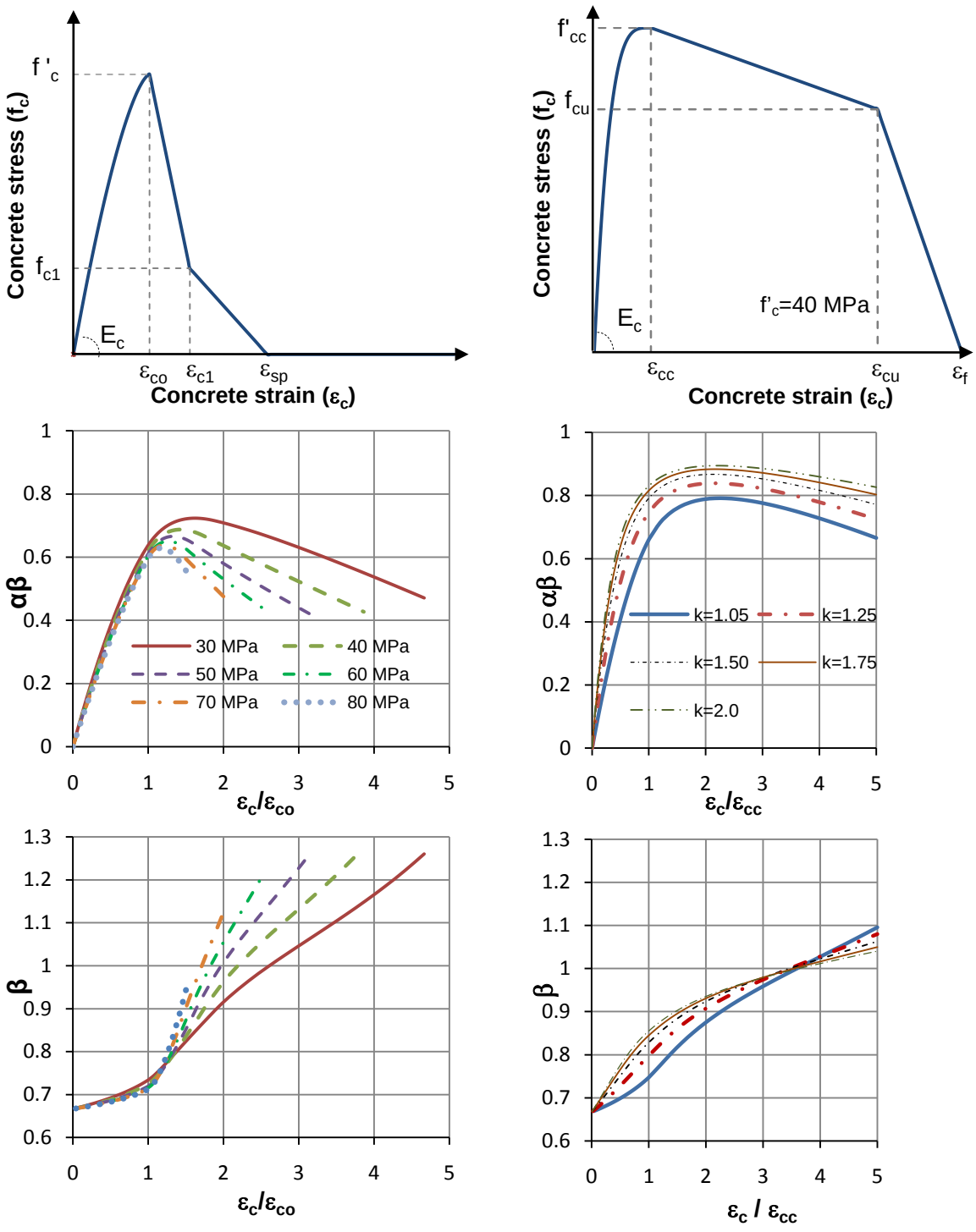

Figure 5: Stress-block parameters for unconfined and confined concrete.

$$\begin{Bmatrix} \Delta P \\ \Delta M \end{Bmatrix}_k = \begin{bmatrix} \frac{\partial P}{\partial \mathcal{E}_o} & \frac{\partial P}{\partial \phi} \\ \frac{\partial M}{\partial \mathcal{E}_o} & \frac{\partial M}{\partial \phi} \end{bmatrix} \begin{Bmatrix} \Delta \mathcal{E}_o \\ \Delta \phi \end{Bmatrix}_k \tag{120}$$

in which the partial derivatives are defined numerically at the beginning of the k^{th} step such that

$$\frac{\partial P}{\partial \mathcal{E}_o} = \frac{P_{k+} - P_k}{\varepsilon_{o\,k+} - \varepsilon_{o\,k}} \tag{121}$$

$$\frac{\partial P}{\partial \phi} = \frac{P_{k++} - P_k}{\phi_{k++} - \phi_k} \tag{122}$$

$$\frac{\partial M}{\partial \mathcal{E}_o} = \frac{M_{k+} - M_k}{\varepsilon_{o\,k+} - \varepsilon_{o\,k}} \tag{123}$$

$$\frac{\partial P}{\partial \phi} = \frac{M_{k++} - M_k}{\phi_{k++} - \phi_k} \tag{124}$$

where $\varepsilon_{o\,k+}$ and ϕ_{k++} are small increments made in strain and curvature to separately find the corresponding changes in axial load and moment.

From the out of balance force remaining from the last solution, $\Delta P = P_{k-1} - N$ along with the increment in curvature (if any), the incremental reference axis strain necessary to restore force equilibrium is given by

$$\Delta\varepsilon_{ok} = \frac{\Delta P - \left(\frac{\partial P}{\partial \phi}\right)_{k-1} \Delta\phi_k}{\left(\frac{\partial P}{\partial \varepsilon}\right)_{k-1}} \tag{125}$$

and the new reference axis strain and corresponding strain profile is obtained as

$$\varepsilon_{ok} = \varepsilon_{ok-1} + \Delta\varepsilon_{ok} \tag{126}$$

$$\varepsilon(y)_k = \varepsilon_{ok} + \phi_k y \tag{127}$$

Step 3: From this the reinforcing bar stresses (130) and stress-block parameters (105) to (112) are found, and the axial load and moment computed as follows

$$P_k = \sum_{i=1}^{n_s} f_{si} A_{si} + \alpha_c \beta_c f'_c \, b_{cov} c_{cov} + \alpha_{cc} \beta_{cc} f'_{cc} \, b_{core} c_{core} \tag{128}$$

$$\mathrm{M_k} = \sum_{i=1}^{n_s} f_{si} A_{si} y_{si} + \alpha_c \beta_c f'_c \, b_{cov} c_{cov} y_c + \alpha_{cc} \beta_{cc} f'_{cc} \, b_{core} c_{core} y_{cc} \tag{129}$$

Step 4: Check the out-of-balance force ($\Delta P = P_{k-1} - N$) is within an acceptable tolerance. If $|\Delta P| <$ tolerance proceed to next curvature value, else set $\Delta \phi = 0$ and go to step 2.

In the analysis of moments and axial loads two different models of the stress-strain performance of the reinforcing steel may be adopted. For nominal design capacities, an elasto-plastic model is customarily adopted to provide a dependable estimate for design. For "exact" analysis of existing reinforced concrete members, a realistic stress-strain model should be adopted using expected values of the control parameters. Such a model (Figure 6), conveniently posed in the form of a single equation is given as:

$$f_s = \frac{E_s \, \varepsilon_s}{\left\{1 + \left|\frac{E_s \, \varepsilon_s}{f_y}\right|^{20}\right\}^{0.05}} + \left(f_{su} - f_y\right)\left[1 - \frac{|\varepsilon_{su} - \varepsilon_s|^P}{\{|\varepsilon_{su} - \varepsilon_{sh}|^{20P} + |\varepsilon_{su} - \varepsilon_s|^{20P}\}^{0.05}}\right] \tag{130}$$

where

$$P = \frac{E_{sh}(\varepsilon_{su} - \varepsilon_{sh})}{\left(f_{su} - f_y\right)} \tag{131}$$

HAND ANALYSIS SOLUTION IMPLEMENTATION

In the hand analysis method using equivalent rectangular stress-block parameters, for a particular value of strain in the extreme concrete fiber of the cover or core concrete the strains at the different levels of steel and the extreme cover and/or core concrete fibers are determined assuming linear distribution of strain along the column cross- section. From the strains the stress-block parameters (α and β) for unconfined and confined concrete and the stresses in steel are calculated. Knowing the area of steel and cover and core concrete, the forces are obtained and an iterative procedure is followed in order to obtain force equilibrium. Ones equilibrium of forces is attained, knowing the depth to the neutral axis of the section from the extreme concrete compression fiber; the moment and curvature are calculated.

NUMERICAL EXAMPLE

Adopting the above procedure for the computational and hand analysis technique, the moment-curvature analysis for a column with an axial load of 2000 kN with the following properties is performed. Section properties: breadth = 600 mm, height = 600 mm, clear cover = 50 mm, length = 1500 mm. Concrete properties: f_c' = 30 MPa, ε_{co} = 0.0019, ε_{sp} = 0.009, f_{cc}' = 45 MPa; ε_{cc} = 0.00675 and E_c = 27387 MPa (the above parameters were calculated using the expressions presented earlier). Reinforcing steel properties: f_y = 430 MPa, E_s = 200000 MPa, f_u = 650 MPa, ε_u = 0.12, ε_{sh} = 0.008, E_{sh} = 8000 MPa, f_{yh} = 430 MPa, diameter of longitudinal bars (d_b) = 25 mm, diameter of stirrups (d_s) = 12 mm and stirrup spacing (s) = 100 mm.

In order to implement the iterative computational procedure to obtain the moment-curvature relation, a MATLAB program was used. The hand computation was performed for the following values of the strain; first yield of steel ε_y, strain at the extreme cover concrete fiber ε_{max} = 0.003, 0.006 and ε_{sp} and strain at the extreme confined concrete fiber $\varepsilon_{max} = \varepsilon_{sp}$ and $2\varepsilon_{cc}$ (Figure 7). The result of the hand computations is presented in (Table 3 through Table 8). A comparison of results is presented in Figure 9.

The differences noted between the proposed model and the classic Mander et al. (1988b) model are ascribed to differences (inaccuracy) in modeling the falling branch of the cover concrete of the latter.

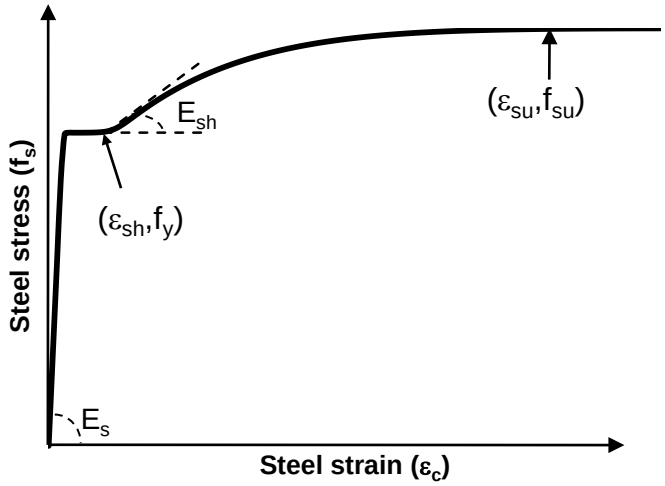

Figure 6: Stress-strain curve for steel.

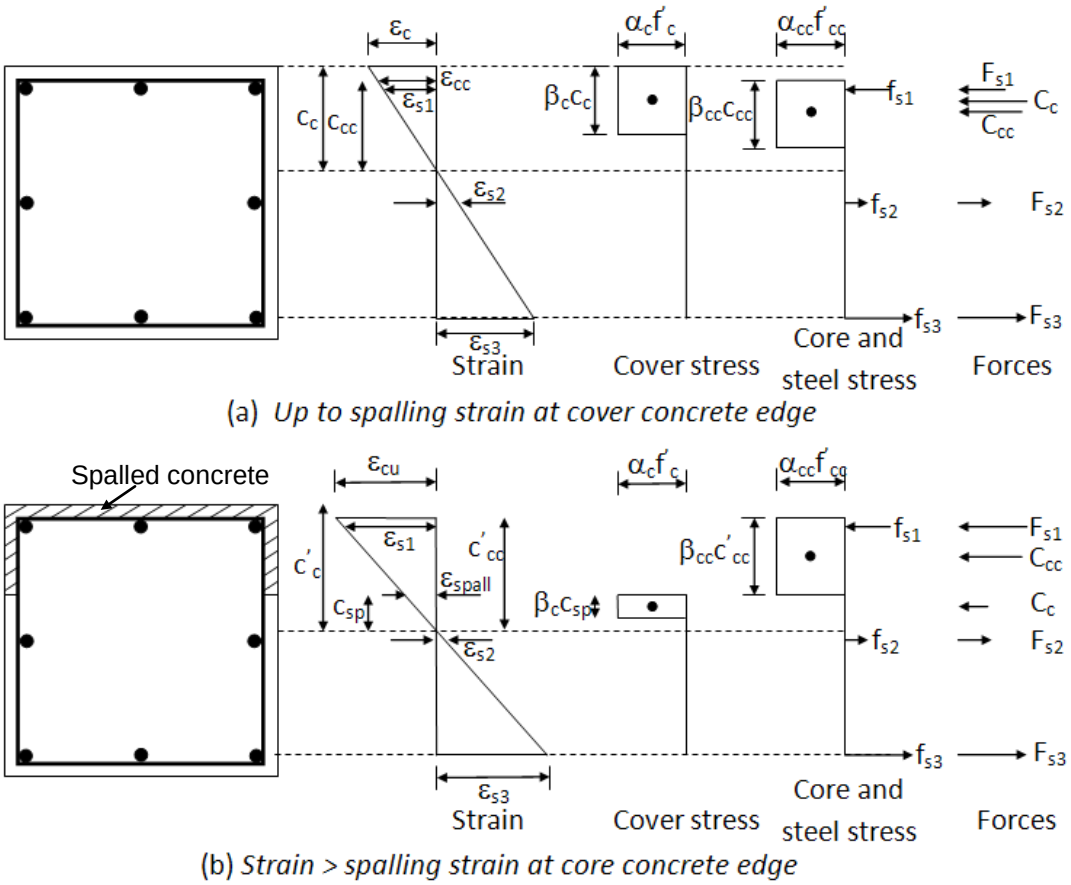

Figure 7: Section strain and stress-block analysis of the cases (a) before and (b) after spalling.

Table 3: Hand computations at yield strain of steel.

Steel		c = -235.10 mm					
Steel layer	Area of steel, mm^2	Strain	Stress MPa		Force kN	Distance from centroid, mm	Moment kN-m
Layer 1	1963.50	-0.0012	-237.89		-467.10	-225.50	105.33
Layer 2	981.75	-0.0001	-15.24		-14.97	-75.17	1.12
Layer 3	981.75	0.0010	207.48		203.69	75.17	15.31
Layer 4	1963.50	0.0022	415.53		815.88	225.50	183.98
Concrete			α	β			
For unconfined concrete	Cover layer	-0.0017	0.8280	0.7238	-2536.0	-214.92	545.04
	Core layer	-0.0013	0.7009	0.7053	1296.2	-180.84	-234.41
For confined concrete		-0.0013	0.4696	0.7017	-1295.95	-181.16	234.78
Curvature	**7.4036E-06**	**ΦD**	**0.0044**	Total	-1998.23		**851.16**

Table 4 : Hand computations at strain =0.003 at cover.

Steel		c = -200.50 mm					
Steel layer	Area of steel, mm^2	Strain	Stress MPa		Force kN	Distance from centroid, mm	Moment kN-m
Layer 1	1963.50	-0.0019	-375.89		-738.06	-225.50	166.43
Layer 2	981.75	0.0004	72.87		71.54	-75.17	-5.38
Layer 3	981.75	0.0026	429.81		421.96	75.17	31.72
Layer 4	1963.50	0.0049	431.10		846.46	225.50	190.88
Concrete			α	β			
For unconfined concrete	Cover layer	-0.0030	0.8164	0.8555	-2520.7	-214.24	540.02
	Core layer	-0.0022	0.8921	0.7537	1422.3	-189.55	-269.60
For confined concrete		-0.0022	0.6540	0.7245	-1503.60	-191.65	288.17
Curvature	**1.50E-05**	**ΦD**	**0.0090**	Total	-2000.04		**942.24**

Table 5 : Hand computations at strain =0.006 at cover.

Steel		c = -193.00 mm					
Steel layer	Area of steel, mm^2	Strain	Stress MPa		Force kN	Distance from centroid, mm	Moment kN-m
Layer 1	1963.50	-0.0037	-430.49		-845.27	-225.50	190.61
Layer 2	981.75	0.0010	198.01		194.39	-75.17	-14.61
Layer 3	981.75	0.0057	431.87		423.99	75.17	31.87
Layer 4	1963.50	0.0103	449.76		883.11	225.50	199.14
Concrete			α	β			
For unconfined concrete	Cover layer	-0.0060	0.4590	1.1425	-1821.9	-189.75	345.70
	Core layer	-0.0043	0.6139	1.0126	1246.8	-174.64	-217.73
For confined concrete		-0.0043	0.8857	0.7809	-2080.79	-190.51	396.41
Curvature	**3.11E-05**	**ΦD**	**0.0187**	Total	-1999.71		**931.38**

Table 6 : Hand computations at spalling strain at cover.

Steel		C = -196.40 mm					
Steel layer	Area of steel, mm^2	Strain	Stress MPa		Force kN	Distance from centroid, mm	Moment kN-m
Layer 1	1963.50	-0.0056	-431.78		-847.79	-225.50	191.18
Layer 2	981.75	0.0013	260.69		255.93	-75.17	-19.24
Layer 3	981.75	0.0082	438.26		430.26	75.17	32.34
Layer 4	1963.50	0.0151	481.42		945.27	225.50	213.16
Concrete			α	β			
Unconfined concrete	Cover layer	-0.0090	0.2898	1.3341	-1366.9	-168.99	231.00
	Core layer	-0.0064	0.4302	1.1691	1033.8	-161.93	-167.41
Confined concrete		-0.0064	0.9570	0.8303	-2449.91	-185.71	454.98
Curvature	**4.58E-05**	**ΦD**	**0.0275**	Total	-1999.32		**936.00**

Table 7 : Hand computations at spalling strain at core.

Steel		c = -200.75 mm					
Steel layer	Area of steel, mm^2	Strain	Stress MPa		Force kN	Distance from centroid, mm	Moment kN-m
Layer 1	1963.50	-0.0078	-436.93		-857.91	-225.50	193.46
Layer 2	981.75	0.0015	299.58		294.11	-75.17	-22.11
Layer 3	981.75	0.0108	453.03		444.76	75.17	33.43
Layer 4	1963.50	0.0202	512.41		1006.12	225.50	226.88
Concrete			α	β			
For unconfined concrete	Cover layer	-0.0090	0.2898	1.3341	-1007.4	-147.44	148.54
	Core layer	-0.0090	0.2898	1.3341	819.4	-147.44	-120.81
For confined concrete		-0.0090	0.9718	0.8736	-2698.73	-180.77	487.86
Curvature	**6.22E-05**	**ΦD**	**0.0373**	Total	-1999.70		**947.25**

Table 8 : Hand computations at maximum core fiber strain of $2\varepsilon_{cc}$.

Steel		c = -205.40 mm					
Steel layer	Area of steel, mm^2	Strain	Stress MPa		Force kN	Distance from centroid, mm	Moment kN-m
Layer 1	1963.50	-0.0118	-459.60		-902.42	-225.50	203.50
Layer 2	981.75	0.0018	351.03		344.63	-75.17	-25.90
Layer 3	981.75	0.0153	483.11		474.29	75.17	35.65
Layer 4	1963.50	0.0289	555.24		1090.21	225.50	245.84
Concrete			α	β			
For unconfined concrete	Cover layer	-0.0090	0.2898	1.3341	-693.2	-127.76	88.57
	Core layer	-0.0090	0.2898	1.3341	563.8	-127.76	-72.03
For confined concrete		-0.0135	0.9475	0.9257	-2877.65	-174.85	503.16
Curvature	**9.04E-05**	**ΦD**	**0.0542**	Total	-2000.35		**978.78**

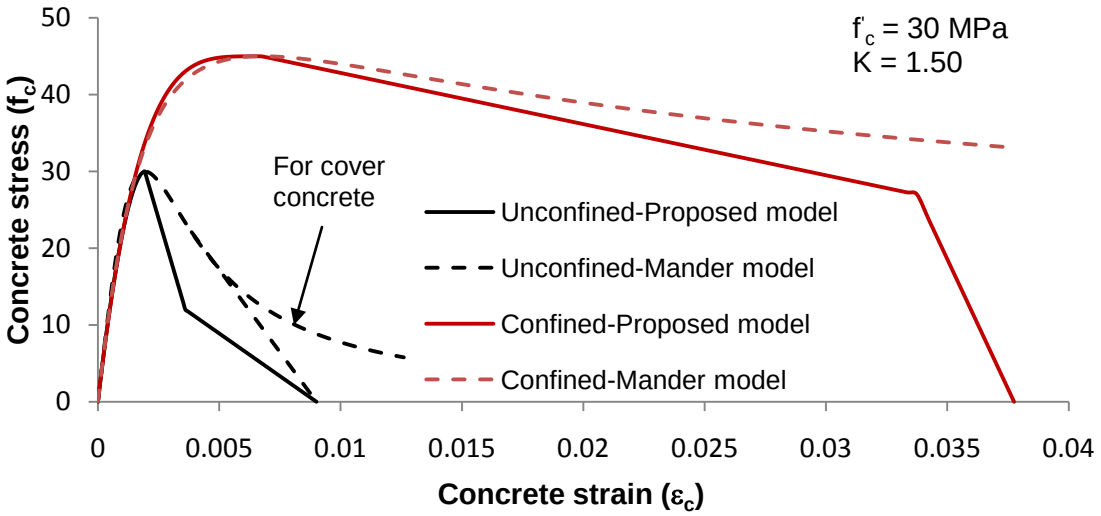

Figure 8: Comparison of proposed and Mander et al. (1988b) stress-strain models.

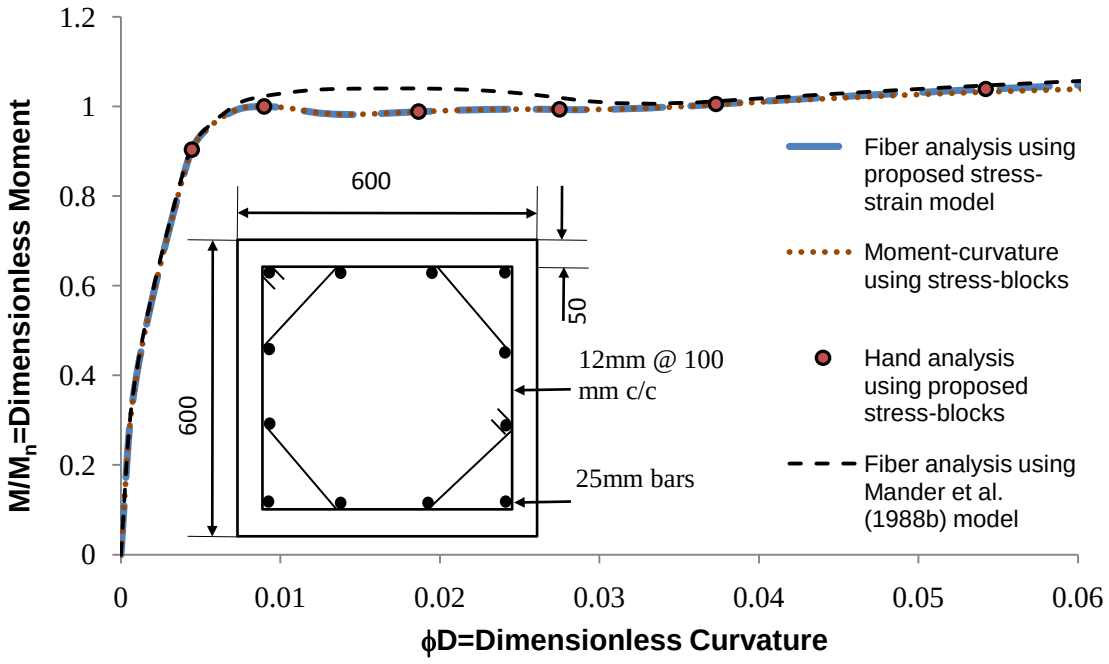

Figure 9: Comparison of moment-curvature results.

3. STRUCTURAL TIMBER-BOXED CONCRETE SYSTEM

3.1 Introduction

Timber is extensively used in the United States for the construction of light-frame residential buildings and apartment complexes because of its eminent advantages of being a light weight material, easy to handle and work with; being aesthetically appealing, reduced environmental impact compared to other construction materials and high thermal efficiency and reduced energy costs for the end user. Timber as a material however, has the disadvantage of being subjected to significant creep, limited to small spans, limited fire-rating, noisy floors and poor sound insulation and may require many walls to stiffen a structure of substantial size. These disadvantages limit the utilization of timber structures in high rise buildings and hence timber structures are usually relegated for use in low rise buildings.

Reinforced concrete, on the other hand, is thought to be stronger, can be used to build longer spans and taller structures; high rise structural concrete buildings in excess of 40 stories have been constructed with no apparent limits. However, these materials are difficult to handle and one requires specialized falsework and formwork equipment systems to work with them. Also, reinforced concrete structures are costlier and may require greater time for construction as compared to timber structures.

In the past two decades extensive studies have been conducted to study the performance of timber-concrete composite structures. The major advantages of this composite construction (Ceccotti 2002) are: lighter structures compared to reinforced

concrete structures, improved load-carrying capacity and structural rigidity over traditional timber floor systems, efficient in terms of load carried per unit self-weight, higher in-plane (diaphragm) rigidity an important feature for performance during earthquakes, relatively highly damped compared to timber systems, superior sound insulation and fire protection compared to timber-only structures, and lower cost and faster construction compared to ordinary reinforced concrete structures. In the case of the composite system used in bridge decks (Mettem 2003) the concrete topping slab protects the timber beneath from direct sun, rain and from wear and tear. The system provides good diaphragm action and better facilitates the distribution of wheel loads amongst the timber stringers.

However, the performance of the timber-concrete composite system depends on the choice of connection system that is used to obtain the composite action. The connections need to be stiff and strong for optimal structural efficiency and at the same time should be economical to obtain overall cost efficiency. By preventing relative slip between the timber beams and concrete topping slabs, the positive aspects of the constituent materials of the composite system can be exploited, with the concrete mainly in compression and the timber in tension and bending.

Composite action between timber and concrete can be obtained by using nails, screws, steel tubes, glued reinforced concrete steel bars, grooves with reinforcing screws and nails and others. Several studies have been conducted in the development of a good

connection system between timber and concrete to obtain a good composite action; but all these connections for composite action lead to significant labor costs for inspection.

Buchanan and Fairweather (1993) studied the seismic performance of glue laminated (gluelam) timber frame buildings. Several types of timber-concrete connections were studied and recommendations made for seismic design. A design procedure was also suggested for low rise multi-story gluelam buildings.

Ceccotti and Fragiacomo (2006) conducted studies on timber-concrete composite beam with glued re-bar connection in outdoor conditions and made recommendations for the evaluation of the connection properties.

Fragiacomo et al. (2007) performed studies on the long-term behavior of composite wood-concrete floor system with shear key connection. The purpose of this study was to popularize the use of the composite timber-concrete system in countries like the United States and United Kingdom where the use of this system is limited. The authors conducted ultimate load tests on the connection detail, ultimate load and long term tests on strips of floor and on full-scale floor/deck systems, and cyclic tests simulating the repetition of the live load during the service life of the structure.

Deam et al. (2007) conducted a pilot study in order to compare the behavior of different connections that can be used in the composite concrete-LVL (laminated veneer lumber) floor system. Based on the study it was concluded that concrete plugs reinforced with screws provided the best stiffness, strength and post-peak behavior of the shear

force-relative slip curve. This improved performance was attributed to the bearing at the interface between LVL and the concrete plug.

Balogh et al. (2008) performed cyclic loading tests on the composite wood-concrete beams with notched connections. A decrease in stiffness and increase in deflection was observed and this was attributed to the progressive damage caused in the connections.

Deam et al. (2008) showed that a LVL-concrete composite system could be used for the construction of medium to long span timber floors. It was shown that there was significant increase in strength and stiffness of the composite beam when compared with bare LVL beams. They also looked into prestressing the composite beam and concluded that though prestressing did not significantly increase the strength or stiffness of the beam, it is beneficial to reduce the mid-span deflections and hence recommended for long-span floor.

Recent studies by Buchanan et al. (2008) have investigated the viability of the construction of multi-story prestressed timber buildings which uses LVL. For the purpose of this study a concrete-timber composite floor system is developed wherein the timber part is prefabricated and the concrete slab is cast in situ. The composite action is obtained between these materials using concrete plugs reinforced with screw based on the results of the pilot study by Deam et al. 2007.

A notable drawback in the composite system is that timber and concrete both exhibit creep under prolonged loading (Clouston et al. 2005) and is a function of applied

stress levels and load duration. For timber, moisture and temperature also influence its creep behavior. Furthermore, concrete shrinks and timber shrinks and swells with variation in temperature. The differential amounts of these characteristics leads to additional demands on the timber-concrete shear connections.

Rather than a strict composite timber-concrete system, this paper presents a study where a conceptual idea of using timber and reinforced concrete as a combined or parallel system is investigated. This system utilizes the positive aspects of both timber and concrete as individual materials and does not need to rely on their composite action and hence does not have any detailed connection requirements. Specifically, the concept is based in the formation of the two main elements of construction: beams (and of course the slabs they support) and columns. Another purpose of this study is to reinvigorate the use of common dimension lumber into economical moment frame construction and also to provide the illusion that the building, although quite tall, is really timber. Concrete is used to strengthen, lengthen and stiffen the mostly timber members. One of the main attributes of timber, its lightness, can essentially be maintained.

3.2 Structural Timber-Boxed Concrete

THE CONCEPT

Concrete structures are formed by casting fresh concrete into timber formwork molds or ‘boxing’. The formwork is held in position by falsework—a false structure that is used to assemble the real structure. Once the concrete cures and hardens, the falsework and formwork are removed and often reused or discarded. The wooden

formwork can be used multiple times but the combined cost of formwork and falsework including the labor cost of erecting and dismantling is a considerable proportion of the final construction cost.

The favorable attributes of timber and concrete are utilized to come up with an innovative and cost effective structural member referred to herein as the *structural timber-boxed concrete* system. In this system, stay-in-place timber formwork is erected on site, some limited reinforcing or prestressing strand is placed and the concrete poured. The formwork is such that it has sufficient strength to support the self-weight of the concrete. Once the concrete has cured, the timber formwork is not removed. The hardened reinforced concrete shares the load with the pre-existing timber structure; combined, they both resist the total factored design loads including transient lateral loads arising from wind and/or seismic effects. The system takes advantage of the structural, architectural, and material advantages of both the materials while combining to form a mixed-material system that offers advantages over other framing systems for comparable use (e.g. cast-in-place concrete).

Apart from the novel idea of using timber, concrete and steel together, the fact that the boxed timber itself acts as the formwork considerably improves and simplifies the construction procedure. The only temporary materials needed are a few lateral bracings and intermediate props (shoring) in order to reduce beam deflections while casting the topping concrete on each floor and these can be reused several times, thus ensuring cost effectiveness. This form of construction is quicker than the conventional

construction and the contractors have the flexibility of immediately occupying the space below the recently finished floor for installation of services as limited shoring exists.

Enormous architectural flexibility is afforded by the structural boxed-concrete system, including various ceiling options (exposed timbers, post-and-beam look, laminated timbers, crown moldings, and easily suspended architectural or acoustical ceilings); the potential for non-structural building systems (electrical, plumbing, HVAC, fiber/cable, lighting, fire suppression system) to be easily installed, accessed, and modified in-service; and options to finish or not finish interior surfaces.

Figure 10 presents the fundamental conceptual idea behind the proposed structural timber-boxed concrete concept. The floor plan of a typical timber-boxed concrete structure is shown with section view of the timber-boxed floor system, column and beam-column joints. Topping mesh is provided in the concrete flooring slab in order to prevent tensile cracking of concrete. The concrete topping is cast over the 2’’x4’’ nail laminated joists. The sequential steps for the construction of the timber-boxed concrete system building would be as follows:

- The boxed-timber columns may be prefabricated (this could be done either at the site by roughing carpenters, or perhaps for a finer finish in a joinery factory).
- The boxed-timber columns would be erected around the previously placed reinforcing cage and plumbed and concrete poured in each of the columns for one floor up to the soffit level of the beams.
- Again, either roughing carpenters or a joinery shop would fabricate the timber-boxed beams. The three-sided timber-boxed beams would be placed and fastened onto

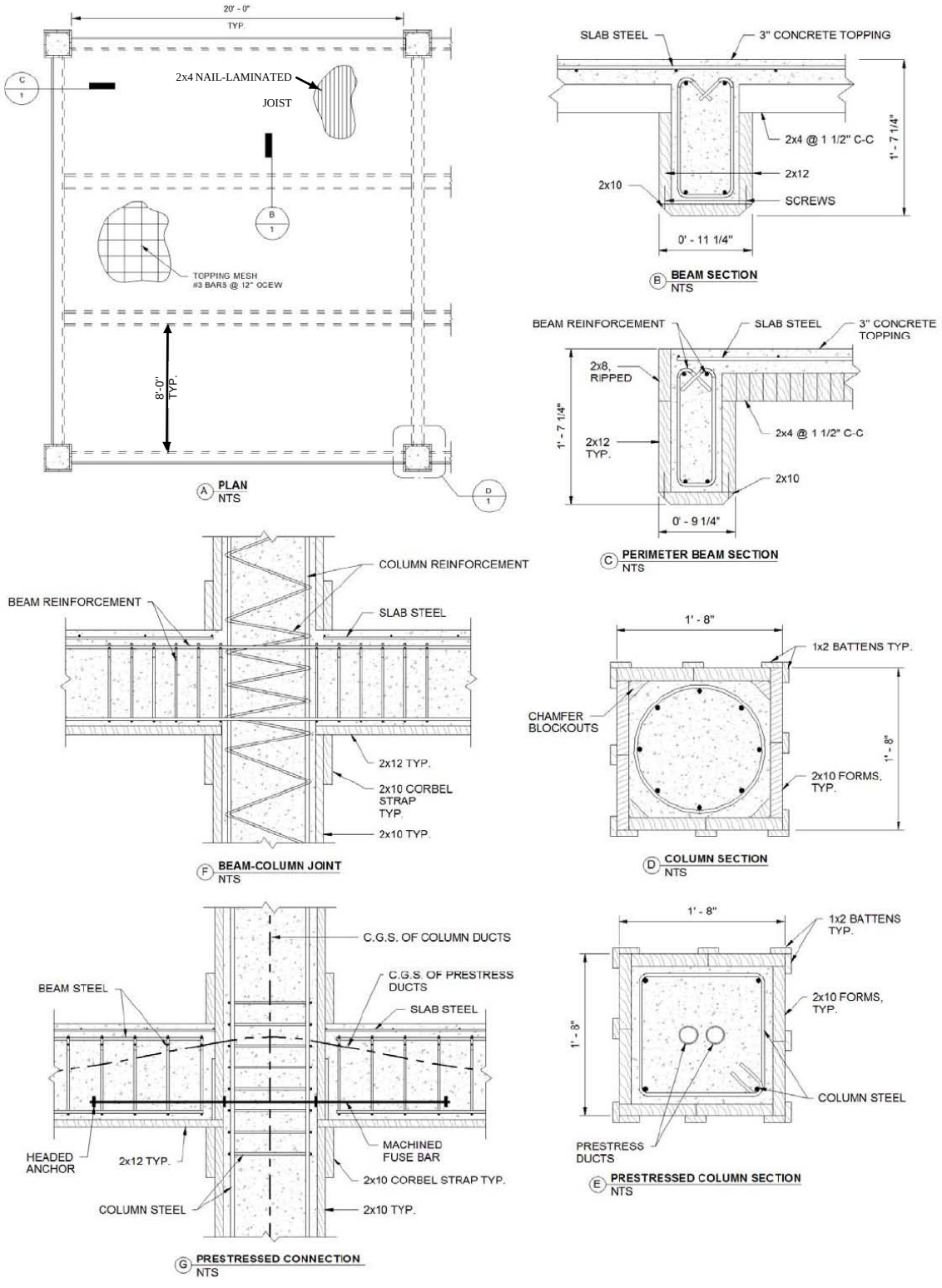

Figure 10: Structural timber-boxed concrete: elements of the concept.
(1 in = 25.4 mm)

timber collars (seats) at the top of the columns, and temporarily propped at the quarter-points (propping would only be required on beams longer than about 6 m).

- The nail-laminated 2”x4” subfloor would then be installed. Once placed this timber sub-floor becomes a strong working surface for all subsequent work.
- Reinforcing cages are then placed within the boxed timber beams and the mesh placed across the timber sub-floor, concrete is poured in the box-beams and floor and left to cure for at least a day.
- Once hardened, the newly finished concrete floor immediately becomes the new working surface for the next story.
- The column reinforcing steel is placed for the next floor and the above procedure is repeated until the building is topped.

Structural timber-boxed concrete, as a combination of two common building materials used in a new way, largely due to its overall lightness, can offer refreshing opportunities for mid-rise and taller construction. In particular, lateral load demands are reduced, leading to further economies. With this approach, there should be no physical limitation on the height of this new class of timber structure.

MATERIAL COMPATIBILITY

A building constructed using the proposed structural timber-boxed concrete system is not a hybrid building, but rather is a mixed (or parallel) material building that relies on favorable properties of the constituent material. When two or more materials are engaged in such a parallel arrangement to perform a structural function, issues of material compatibility arise. Since this is a layered system which really does not rely on

composite action, the issues are fewer. However, proper consideration needs to be given to differential creep, shrinkage (and swell), changes in strength and stiffness with time, and differences in response to moisture between the timber and concrete materials. Properly understood, it is expected that proper detailing can compensate effectively for these material differences.

The high variability of timber strength in the connection regions can result in brittle failure of the composite timber-concrete system. However, the use of wood-based engineered materials like laminated veneer lumber and glued laminated timber has shown to give better performance for composite timber-concrete members when compared to dimension/stick lumber because of their improved strength, dimensional stability and uniformity. Though these products show improved strength, they do not show significant improvement in stiffness and these engineered timber materials considerably increase the cost – typically at least twice that of ordinary dimension lumber. As the proposed system does not rely on composite action, construction grade treated and untreated dimensioned lumber is used; this is readily available and considered less costly, thus improving the overall economy of the system.

One way of overcoming a primary unfavorable attribute of creep deflections in combined timber and concrete systems is to incorporate a load-balancing prestressed system. If dead loads are balanced with judicious use of post-tensioned prestress applied through draped ducts embedded in the concrete, then only axial compression stresses will exist in the materials – as dead deflections are zero, there will be no associated creep deflections. With long-term creep deflections being negated this should help overcome

much of the differential creep problem, as only short-term (non-creep associated) deflections exist.

Another potentially unfavorable attribute is the migration of moisture between the component materials: timber and concrete. For example, if the timber is kiln-dried, then there will likely be migration of moisture from the green concrete into the timber. This causes the concrete to shrink, while the timber would swell. Conversely, if a relatively low water/cement ratio concrete mix is poured into the timber boxing, both the timber and the concrete would dry out, but the timber would shrink more than the concrete. As the concrete would inhibit substantial shrinking of the timber, the timber would end up splitting longitudinally (parallel to the grain). To overcome these issues, several approaches could be adopted, from coating the inside of the boxes prior to casting the concrete, to providing a physical moisture barrier in the form of a polythene sheet. It is expected that the former may be appropriate for beams and columns, while the latter would be more suitable for the casting of the floor slabs. Finally, the mode in which dimensioned lumber is used in the proposed system will permit the use of some off-grade (lower grade) material

3.3 Strength and Deformation Analysis for Design

Prior to building timber-boxed concrete structural elements for the purpose of experimental testing, it is first necessary to develop suitable simple design theories. These shall be based upon extending existing strength-based equilibrium and compatibility models that use stress-blocks for reinforced concrete in compression. The

extension shall primarily consist of using strain amplitude dependent stress-blocks for timber in both tension and compression.

For this purpose it is necessary to have constitutive stress-strain relations for unconfined concrete, timber and reinforcing steel. From the constitutive stress-strain relation for concrete and timber the stress-block parameters can be obtained. As is presently done for reinforced concrete, it is proposed to use a stress-block approach to perform strength and moment-curvature analysis to study the strength and ductility capacities of these structural members.

In this study the stress-strain models for unconfined concrete and reinforcing steel proposed in section 2 are used (Figure 3 and Figure 6). The model for unconfined concrete will now be adapted for use in timber.

STRESS-STRAIN MODEL FOR TIMBER

For performing an analytical moment-curvature analysis on the timber-boxed concrete system it is necessary to have a stress-strain model for timber. Figure 11 presents the proposed stress-strain relation for timber, an adaptation of the stress-strain model proposed for unconfined concrete in section 2, consisting of an initial power curve up to the peak stress, followed by a bilinear relation in the post-peak region. The stress-strain model for timber in tension and compression is set by three coordinates: the peak strength, reduced post-peak capacity and failure strain given by $(\varepsilon_{tow}, f'_{tw})$, $(\varepsilon_{t1w},\ f_{t1w})$ and (ε_{sptw}) for timber in tension and $(\varepsilon_{cow}, f'_{cw})$, $(\varepsilon_{c1w}, f_{c1w})$ and (ε_{spcw}) for timber in compression.

The expressions representing the proposed stress-strain relation for timber in compression are presented below.

$0 \leq x < 1$ $$f_w = f'_{cw}(1 - |1 - x|^n) \quad (132)$$

$1 \leq x < x_u$ $$f_w = f'_{cw} - (f'_{cw} - f_{c1w})\left(\frac{x-1}{x_u - 1}\right) \quad (133)$$

$x_u \leq x < x_f$ $$f_{\mathrm{w}} = f_{c1w}\left(\frac{x - x_{\mathrm{f}}}{x_u - x_f}\right) \quad (134)$$

in which $x = \frac{\varepsilon_w}{\varepsilon_{cow}}$, $x_u = \frac{\varepsilon_{c1w}}{\varepsilon_{cow}}$ and $x_f = \frac{\varepsilon_{spcw}}{\varepsilon_{cow}}$. The term *n* is given by

$$n = \frac{E_{cw}\ \varepsilon_{cow}}{f'_{cw}} \quad (135)$$

where ε_w and f_w is the strain and stress in timber and E_{cw} is the modulus of elasticity of timber in compression. For timber in tension the terms $(\varepsilon_{cow}, f'_{cw})$, $(\varepsilon_{c1w},\ f_{c1w})$, (ε_{spcw}) and E_{cw} in the above equations are replaced by $(\varepsilon_{tow}, f'_{tw})$, $(\varepsilon_{t1w}, f_{t1w})$, (ε_{sptw}) and E_{tw} (modulus of elasticity of timber in tension) respectively.

In this study the following values of the controlling parameters for the stress-strain model for timber are used as obtained from experimental data reported in Shama and Mander (2004). f'_{cw} = 50 MPa, ε_{cow} = 0.005, f_{c1w} = 30 MPa, ε_{c1w} = 0.012, ε_{spcw} = 0.15, E_{cw} = 10700 MPa, f'_{tw} = 40 MPa, ε_{tow} = 0.005, f_{t1w} = 20 MPa, ε_{t1w} = 0.0075, ε_{sptw} = 0.01 and E_{tw} = 9000 MPa.

The proposed stress-strain model for timber in tension and compression is validated against experimental results from tests conducted parallel to the grain on *New Zealand Pinus Radiata* by Rahardjo (2004) and on *Douglas Fir* by Shama and Mander

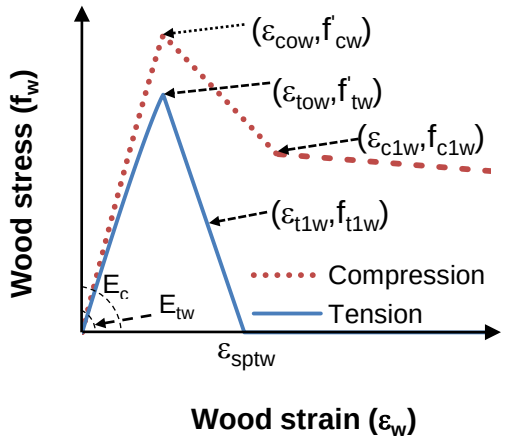

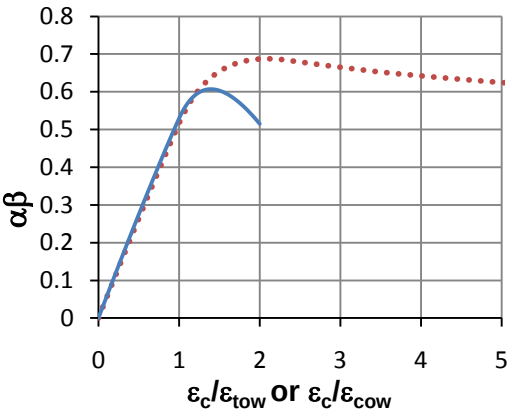

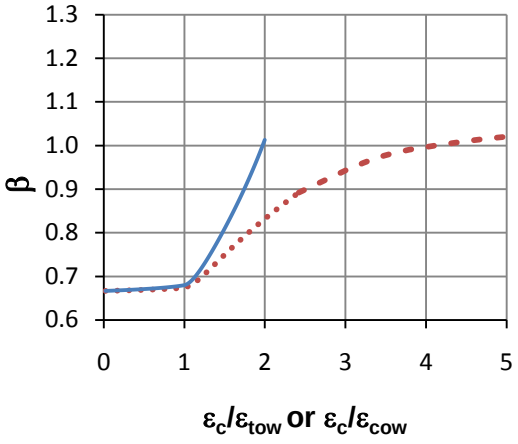

Figure 11: Stress-strain model and stress-block parameters for wood.

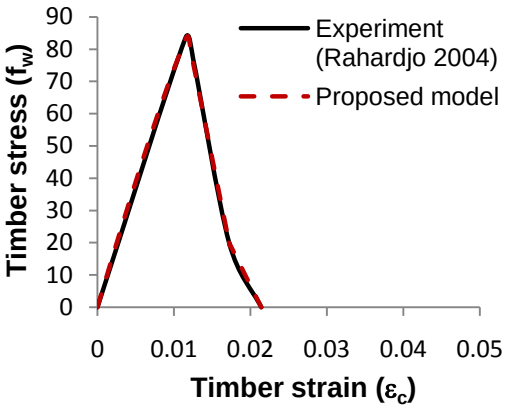

(a) Tension parallel to grain of New Zealand Pinus Radiata

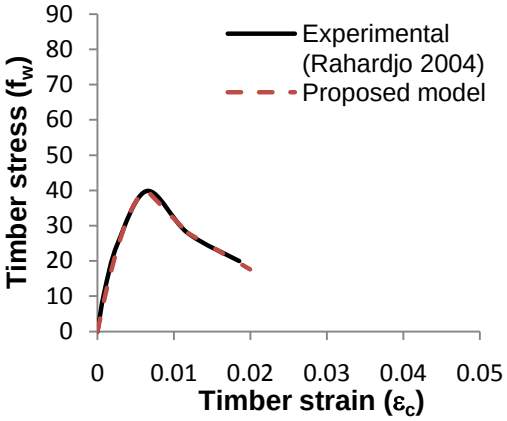

(b) Compression parallel to grain of New Zealand Pinus Radiata

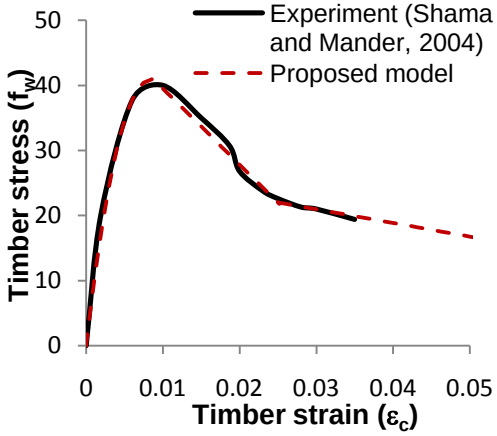

(c)Compression parallel to grain of Douglas Fir

Figure 12: Comparison of stress-strain relationship of timber using proposed model and experimental results.

(2004). Figure 12 shows a comparison of the experimental results and the proposed stress-strain model; good agreement between the two is evident.

STRESS-BLOCK APPROACH

Equivalent rectangular stress-block parameters are extensively used in the analysis and design of concrete structural members and offer a convenient way to determine their capacity. In this study it is proposed to use the stress-block approach to perform the analytical moment-curvature analysis of the timber-boxed concrete members. For this purpose it is necessary to obtain the equivalent rectangular stress-block parameters for both concrete and timber. The stress-block parameters are derived from the stress-strain relation of the materials. The stress-block parameters for unconfined concrete can be found in section 2.

EQUIVALENT RECTANGULAR STRESS-BLOCK PARAMETERS FOR TIMBER

The idea of using equivalent rectangular stress-block parameters for analysis is extended to timber. In order to determine the stress-block parameters, the effective average timber stress ratio (α) and the effective stress-block depth factor (β), the area and the first moment of area under the stress-strain curve of timber and the effective rectangular stress-block are equated and is given by

$$A_c = \int_0^{\varepsilon_c} f_c \, d\varepsilon_c = \alpha \, f_c' \, \beta \, \varepsilon_c \tag{136}$$

$$A\bar{y} = \int_0^{\varepsilon_c} f_c \, \varepsilon_c d\varepsilon_c = \left(1 - \frac{\beta}{2}\right) \varepsilon_c \int_0^{\varepsilon_c} f_c \, d\varepsilon_c \tag{137}$$

from which the stress-block parameters can be found from

$$\alpha\beta = \frac{\int_0^{\varepsilon_c} f_c \, d\varepsilon_c}{f_c' \varepsilon_c} \tag{138}$$

and (139)

$$\beta = 2 - 2\frac{\int_0^{\varepsilon_c} f_c \varepsilon_c d\varepsilon_c}{\varepsilon_c \int_0^{\varepsilon_c} f_c d\varepsilon_c}$$

Carrying out the integration in (138) and (139) using the stress-strain relations (132) to (134) gives the stress-block relations as follows.

i. For $0 \leq x < 1$

$$\alpha\beta = 1 + \frac{(1-x)^{n+1} - 1}{x(n+1)} \tag{140}$$

$$\beta = 2 - \frac{2}{x^2 \alpha\beta}\left[\frac{x^2}{2} + \frac{x(1-x)^{n+1}}{(n+1)} + \frac{(1-x)^{n+2} - 1}{(n+1)(n+2)}\right] \tag{141}$$

ii. For $1 \leq x < x_{cu}$

$$\alpha\beta = \frac{A_1}{x} + \frac{x-1}{x}\left[1 + \left(\frac{f_{c1w} - f_{cw}'}{2f_{cw}'}\right)\left(\frac{x-1}{x_u - 1}\right)\right] \tag{142}$$

$$\beta = 2 - \frac{1}{x^2 \alpha\beta}\left[B_1 + (x^2 - 1) + \frac{(f_{c1w} - f_{cw}')}{3f_{cw}'}\left(\frac{2x^3 - 3x^2 + 1}{x_u - 1}\right)\right] \tag{143}$$

iii. For $x_u \leq x < x_f$

$$\alpha\beta = \frac{A_1}{x} + \frac{A_2}{x} + \frac{f_{c1w}}{2f'_{cw}}\left(\frac{(x - x_u)\left(x + x_u - 2x_f\right)}{x\left(x_u - x_f\right)}\right) \tag{144}$$

$$\beta = 2 - \frac{1}{x^2\alpha\beta}\left[B_1 + B_2 + B_3 + \frac{f_{c1w}}{3f'_{cw}}\left(\frac{3x_f {x_u}^2 - 2{x_u}^3 + x^2\left(2x - 3x_f\right)}{x_u - x_f}\right)\right] \tag{145}$$

iv. For $x \geq x_f$

$$\alpha\beta = \frac{A_1}{x} + \frac{A_2}{x} + \frac{f_{c1w}}{2f'_{cw}}\left(\frac{x_f - x_u}{x}\right) \tag{146}$$

$$\beta = 2 - \frac{B_1 + B_2 + B_3 + B_4}{x^2\alpha\beta} \tag{147}$$

In the above the following coefficients are used

$$A_1 = \frac{n}{(n+1)} \tag{148}$$

$$A_2 = \left(\frac{x_u - 1}{2}\right)\left(1 + \frac{f_{c1w}}{f'_{cw}}\right) \tag{149}$$

$$B_1 = \frac{n(n+3)}{(n+1)(n+2)} \tag{150}$$

$$B_2 = ({x_u}^2 - 1) \tag{151}$$

$$B_3 = \left(\frac{f_{c1w} - f'_{cw}}{3f'_{cw}}\right)\left(\frac{2{x_u}^3 - 3{x_u}^2 + 1}{x_u - 1}\right) \tag{152}$$

$$B_4 = \frac{f_{c1w}}{3f'_{cw}}\left(\frac{3x_f {x_u}^2 - 2{x_u}^3 - {x_f}^3}{x_u - x_f}\right) \tag{153}$$

in which $x = \frac{\varepsilon_w}{\varepsilon_{cow}}$, $x_u = \frac{\varepsilon_{c1w}}{\varepsilon_{cow}}$ and $x_f = \frac{\varepsilon_{spcw}}{\varepsilon_{cow}}$.

The stress-block parameters, α and β, for timber are shown in the lower two graphs of Figure 11. From the plots for stress-block parameters for timber, it can be noted that timber exhibits a linear elastic behavior in both tension and compression up to

strains corresponding to maximum timber strength. For nominal strength design of timber structural elements the value of α = 0.80 and β = 0.67 are suggested.

3.4 Analytical Studies

TIMBER-BOX CONCRETE COLUMN STRENGTH AND BEHAVIOR

Figure 10E shows the cross-sectional details of a timber-boxed concrete column. An analytical moment-curvature analysis using stress-block parameters for concrete and timber is performed on the structural timber-boxed concrete column in order to evaluate its performance as compared to the conventional reinforced concrete members. The following properties were used for the analysis. Column section properties: breadth = depth = 500 mm, clear cover = 25 mm. Concrete properties (refer Figure 3): f_c' = 30 MPa, ε_{co} = 0.002, ε_{c1} = 0.0036, f_{c1} = 12 MPa, ε_{sp} = 0.007 and E_c = 27000 MPa. Timber properties (refer Figure 11): f_{cw}' = 50 MPa, ε_{cow} = 0.005, f_{c1w} = 30 MPa, ε_{c1w} = 0.012, ε_{spcw} = 0.15, E_{cw} = 10700 MPa, f_{tw}' = 40 MPa, ε_{tow} = 0.005, f_{t1w} = 20 MPa, ε_{t1w} = 0.0075, ε_{sptw} = 0.01 and E_{tw} = 9000 MPa. Longitudinal reinforcing steel properties (refer Figure 6): f_y = 430 MPa, E_s = 200000 MPa, f_u = 650 MPa, ε_u = 0.12, ε_{sh} = 0.012, E_{sh} = 8000 MPa and diameter of longitudinal bars d_b = 25 mm; for transverse steel: yield strength f_{yh} = 430 MPa, diameter d_s = 12 mm and stirrup spacing s = 100 mm.

For the analysis of the timber-boxed concrete column shown in Figure 10E several conditions are considered, as follows:

(a) Tension and compression in timber are considered for column sections corresponding within the mid-height region of the member. Thus, because of symmetry, strain compatibility between the materials can be assumed.

(b) At the fixed ends of the column member, refer to Figure 10F, the timber is discontinuous through the beam-column joint. Thus the timber can only contribute in compression.

(c) For sake of completeness, results are shown for the 4-bar and 8-bar reinforced concrete columns (neglecting the beneficial effects of the timber).

Figure 13 presents the results for (a) axial-load moment interaction and in (b) and (c) moment-curvature analysis for two different axial loads 1000 and 2500 kN. From the axial-load moment interaction diagram in Figure 13a it can be seen that the contribution of timber in tension and compression within the mid-height of the timber-boxed concrete column increases the moment-capacity by as much as three times when compared to the reinforced concrete only column. It is also observed that at the fixed ends of the column member, where the timber contributes in compression only, the moment capacity of the timber-boxed concrete is higher than the reinforced concrete only column and this trend increases with the increase in axial-loads. From Figure 13(b) and (c) it is seen that the timber-boxed concrete columns show greater ductility when compared to the reinforced concrete only section.

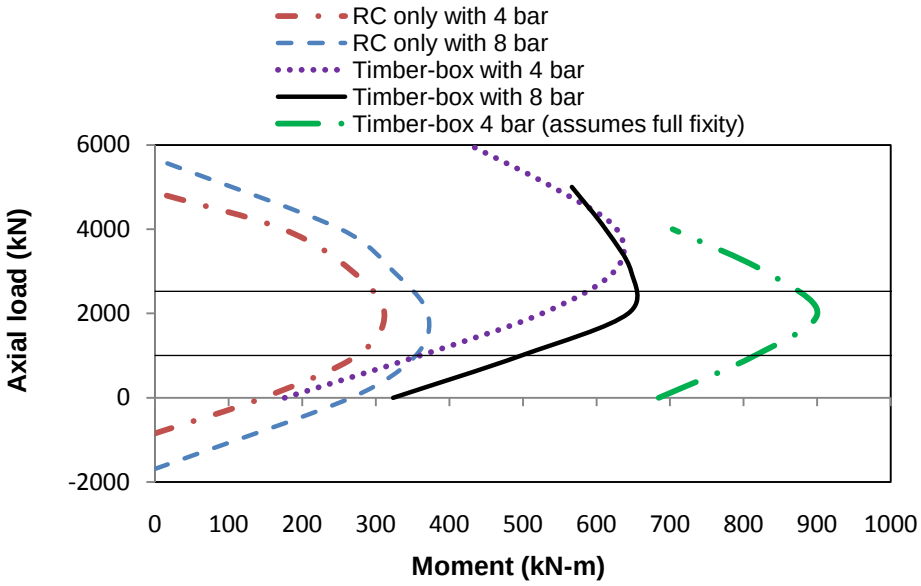

(a) Moment vs. axial load interaction

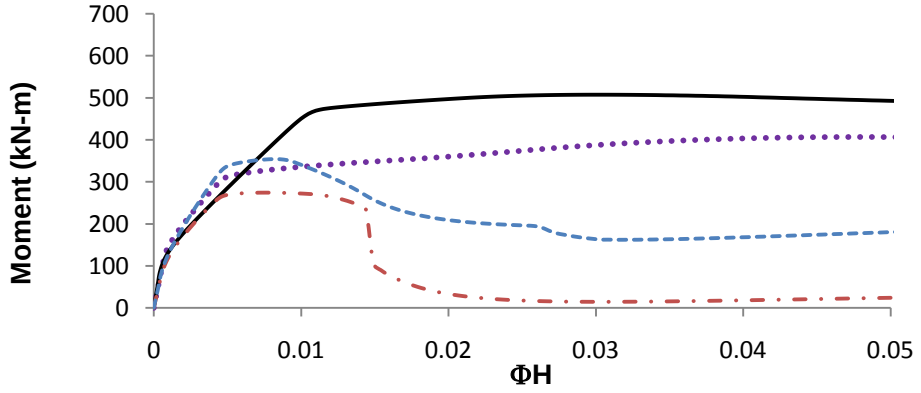

(a) Moment vs. curvature for P=1000 kN

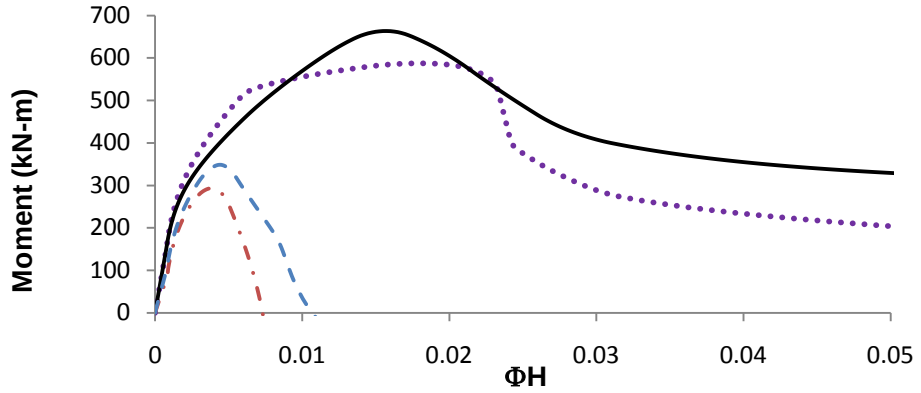

(c) Moment vs. curvature for P=2500 kN

Figure 13: Relative strength of timber-boxed concrete vs. reinforced concrete only columns.

TIMBER-BOX CONCRETE T-BEAM STRENGTH AND BEHAVIOR

Figure 10B shows the cross-sectional details for the timber-boxed concrete T-beam. An analytical stress-block based moment-curvature analysis is performed for the timber-boxed concrete and reinforced concrete only T-beam in order to compare their capacities. The section properties of the secondary T-beam in the east-west direction are: topping slab breadth = 2.44 m, thickness of concrete topping = 75 mm, slab reinforcement = 10 mm reinforcing bars at 300 mm spacing, total section depth = 490 mm, breadth of boxed beam section = 285 mm and beam reinforcement = 25 mm bars. Other properties remaining the same, the section properties for the primary T-beam in the north-south direction are: total section depth = 590 mm and breadth of boxed beam section = 275 mm The concrete, reinforcing steel and timber properties are the same as that used for the column listed above. The analysis is performed for the following three cases for positive and negative moments.

(a) Timber tension and compression are considered for the timber-boxed concrete T-beam section within the mid-length region of the member.
(b) Compression alone is considered at the beam-column joints where the timber is discontinuous.
(c) A reinforced concrete only section without any timber.

Figure 14a shows the moment-curvature analysis results for the east-west secondary T-beam where the participation of the timber flooring is not considered. In this case, for positive moments within the mid-length of the section, there is an increase

in moment capacity at small curvatures, but the behavior is similar to reinforced concrete only system at higher curvatures making the timber ineffective at large curvatures. It is also observed that timber is ineffectual at the end spans where, due to discontinuities, the timber contribution is only in compression. In the case of negative moments, the timber-boxed concrete T-beam shows greater strength compared to the reinforced concrete only members.

Figure 14b represents the moment-curvature analysis results for the primary T-beam in the north-south direction considering the timber flooring to participate. The results are similar to the secondary beam in the east-west direction; however it is to be noted that the timber flooring contributes towards increasing the moment capacity of the primary T-beams by about 30 percent, compared to the secondary T-beams.

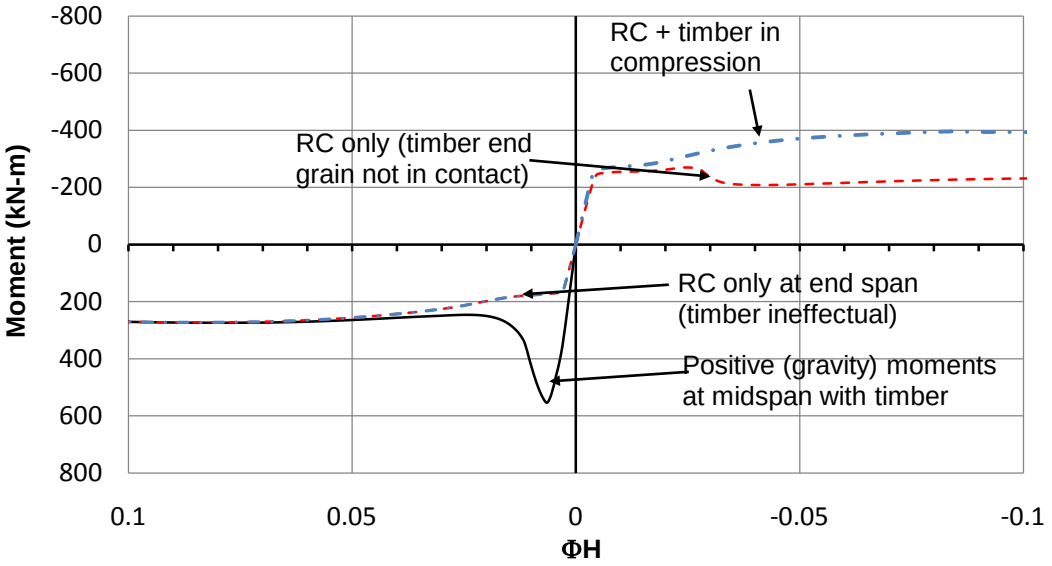

(a) East-west secondary T-beam (timber flooring does not participate)

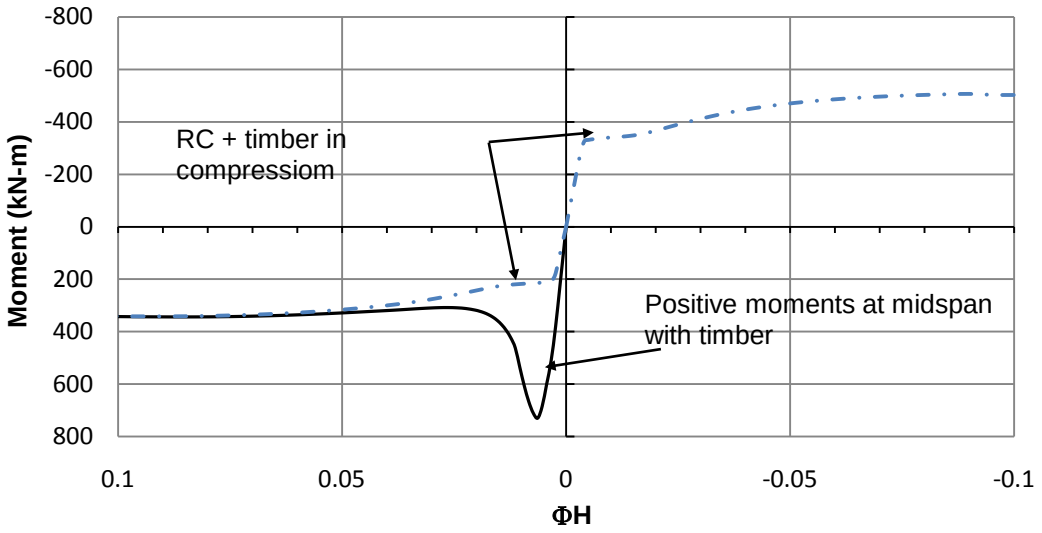

(b) North-south primary T-beam (timber flooring participates)

Figure 14: Relative strength of timber-boxed concrete vs. reinforced concrete only floor system.

4. SUMMARY, CONCLUSIONS AND RECOMMENDATIONS

4.1 Summary

This study was primarily concerned about modeling a simple stress-strain relation for both unconfined and confined concrete which can represent the behavior of normal-strength and high-strength concrete. The proposed stress-strain model overcomes a major shortcoming of the existing concrete stress-strain models which either do not represent the falling branch of the stress-strain relation properly or cannot be easily inverted or integrated to determine the equivalent rectangular stress-block parameters.

A stress-strain relation was proposed for both unconfined and confined concrete. The model was defined by a simple power curve for the ascending branch and bilinear straight line equations for the post-peak behavior. The nature of the curves allowed the stress-strain relations to be easily inverted and readily integrated to determine the equivalent rectangular stress-block parameters.

The proposed stress-strain model was found to well represent the experimental and analytical results for the columns tested and analyzed by Mander et al. (1988b). The computational moment-curvature result that was obtained by performing a fiber-analysis using the proposed stress-strain model of unconfined and confined concrete and the stress-block analysis were found to match well with the results obtained from the fiber analysis using Mander et al. (1988b) model. The difference at the peak was due to the difference in the falling branch of the cover concrete stress-strain model, which is steeper for the proposed model.

Closed form expressions were derived for the equivalent rectangular stress-block parameters and a hand analysis was performed using these. The hand computation results had a good match to the moment-curvature results from the computational fiber and stress-block analysis and can provide as an easy method for design checks.

Empirical relations were also derived for the various controlling parameters of the stress-strain model. This enables one to obtain the stress-strain relation of both unconfined and confined concrete in the absence of accurate experimental data.

A conceptual idea for the use of dimensioned lumber and reinforced concrete as a parallel system in order to build an efficient and economic system referred to as timber-boxed concrete was developed. The system need not rely on composite action between timber and reinforced concrete, rather the system acts like a parallel or mixed system utilizing the positive aspects of all the constituent materials.

In order to perform a stress-block based moment-curvature analysis on the timber-boxed concrete section, a stress-strain model for timber is proposed and the stress-blocks for timber are derived from these.

The rectangular stress-block parameters that were developed for timber and unconfined concrete were incorporated in a computer program in order to obtain the moment-curvature plot of the timber-boxed concrete and ordinary reinforced concrete columns and T-beam. With this analysis the moment capacities of the sections were compared.

4.2 Conclusions

The following are the major conclusions from this study:

i. The proposed stress-strain relation of concrete well represents the behavior of both normal strength and high strength concrete in their unconfined and confined states.

ii. The proposed stress-strain relation can be easily inverted and conveniently integrated.

iii. By equating the area and the first moment of area under the stress-strain curve and an equivalent rectangular stress-block, closed form relation for the stress-block parameters are obtained.

iv. The stress-strain relations are controlled by a few controlling parameters and empirical expressions for these parameters based on f_c' are derived so that these relations can be used in the absence of accurate experimental results.

v. A stress-block hand analysis approach using the derived equivalent rectangular stress-block parameters can be performed in order to obtain the moment-curvature relation for reinforced concrete members.

vi. The concept of the proposed stress-strain model for unconfined concrete is extended to timber in order to obtain a stress-strain relation and is found to be well representative of the experimental results.

vii. Expressions for rectangular stress-block parameters for timber are obtained and the stress-block approach extended to timber. Values of stress-block

parameters, α = 0.80 and β = 0.67 are recommended to be used for nominal strength design of timber

viii. A concept of timber-boxed concrete is developed and the moment-curvature relations of these structural systems are determined using the stress-block parameters.

ix. Height limitations of timber structures can be overcome and construction cost and time reduced due to reduced formwork.

x. The results from the preliminary analysis show good promise for the application of the proposed timber-boxed concrete system.

4.3 Recommendations for Further Work

This section outlines a few important areas in which further studies is essential.

i. Tests to calibrate the stress-strain model of timber with tests on dimensioned lumber and propose empirical relations for the mechanical properties of timber.

ii. Experimental investigation to verify the analytical results of timber-boxed concrete structural members and propose new theories to support the experimental work, if required.

iii. Study performance of the boxed concrete system under static and dynamic loading and also long-term behavior of this system.

iv. The fire rating of the proposed dual system also needs to be investigated.

REFERENCES

ACI Committee 318, "Building code requirements for structural concrete (318-05) and commentary-(318R-05)." ACI, Farmington Hills, Michigan, 2005.

Azizinamini, A., Kuska, S., Brungardt, P., and Hatfield, E. (1994). "Seismic behavior of square high strength concrete columns." *ACI Structural Journal*, 91(3), 336-345.

Attard, M.M., and Steward, M.G. (1998). "A two parameter stress-block for high-strength concrete." *ACI Structural Journal*, 95(3), 305-317.

Balogh, J., Fragiacomo, M., Gutkowski, R.M., and Fast, R.S. (2008). "Influence of repeated and sustained loading on the performance of layered wood-concrete composite beams. " *J. Struct. Eng.* 134(3), 430-439.

Bjerkeli, L., Tomaszewicz, A., and Jensen, J.J. (1990). "Deformation properties and ductility of high-strength concrete." *High-Strength Concrete: Second International Symposium*, American Concrete Institute, Detroit, MI., 215-238.

Buchanan, A., and Fairweather, R.H. (1993). “Seismic design of glulam structures.” *Bulletin of the New Zealand National Society for Earthquake Engineering*, 26(4), 415-436.

Buchanan, A., Deam, B., Fragiacomo, M., Pampanin, S., and Palermo, A. (2008). "Multi-story prestressed timber building in New Zealand" *Structural Engineering International*, 18(2), 166-173.

Ceccotti, A., (2002). "Composite concrete-timber structures." *Progress in Structural Engineering and Materials*, 4(3), 264-275.

Ceccotti, A., and Fragiacomo, M. (2006). "Long term and collapse tests on a timber-concrete composite beam with glued-in connection." *Materials and Structures*, 40(1), 15-25.

Clouston, P., Bathon, L.A., and Schreyer, A. (2005). "Shear and bending performance of a novel wood-concrete composite system." *Materials and Structures*, 131(9), 1404-1412.

Deam, B.L., Fragiacomo, M., and Buchanan, A.H. (2007). "Connections of composite concrete slab and LVL flooring system." *Materials and Structures*, 41(3), 495-507.

Deam, B.L., Fragiacomo, M., and Shane Gross, L. (2008). "Experimental behavior of prestresses LVL-concrete composite beams." *J. Struct. Eng.*, 134(5), 801-809.

Desayi, P., Iyengar, K.T.S.A., and Reddy, T.S. (1978). "Equation for stress-strain curve of concrete confined in circular steel spiral." *Materials and Structures*, 11(65), 339-345.

Fragiacomo, M., Gutkowski, R.M., Balogh, J., and Fast, R.S. (2007). "Long-term behavior of wood-concrete composite floor/deck systems with shear key connection detail. " *J. Struct. Eng.* 133(9), 1307-1315.

Hognestad, E. (1951). "A study on combined bending and axial load in reinforced concrete members." Univ. of Illinois Engineering Experiment Station, Univ. of Illinois at Urbana-Champaign, IL, 43-46.

Ibrahim, H.H.H., and MacGregor, J.G. (1997). "Modification of the ACI rectangular stress block for high-strength concrete." *ACI Structural Journal*, 94(1), 40-48.

Kent, D.C., and Park, R. (1971). "Flexural members with confined concrete." *Journal of the Structural Division, Proc. of the American Society of Civil Engineers*, 97(ST7), 1969-1990.

Li, B., Park, R., and Tanaka, H. (2000). "Constitutive behavior of high-strength concrete under dynamic loads." *ACI Structural Journal*, 97(4), 619-629.

Li, B., Park, R., and Tanaka, H. (2001). "Stress-strain behavior of high-strength concrete confined by ultra-high and normal-strength transverse reinforcements." *ACI Structural Journal*, 98(3), 395-406.

Mander, J.B. (1983). "Seismic design of bridge piers." Ph.D Thesis, Univ. of Canterbury, New Zealand.

Mander, J.B., Priestley, M.J., and Park, R. (1988a) "Observed stress-strain behavior of confined concrete." *J. Struct. Eng.*, 114(8), 1827-1849.

Mander, J.B., Priestley, M.J.N., and Park, R. (1988b) "Theoretical stress-strain model of confined concrete." *J. Struct. Eng.*,114(8), 1804-1826.

Mettem, C. (2003). "Structural timber-concrete composites – advantages of a little known innovation." *The Structural Engineer*, 81(4), 17-19.

Park, R., and Paulay, T. (1975). *Reinforced concrete structures*, John Wiley and Sons, New York.

Popovics, S. (1973). "A numerical approach to the complete stress-strain curves of concrete." *Cement and Concrete Research*, 3(5), 583-599.

Rahardjo, T. (2004). "Experiments and stochastic modelling of New Zealand grown Pinus Radiata timber and timber piles under seismic loading." ME Thesis, University of Canterbury, New Zealand.

Roy, H.E.H., and Sozen, M.A. (1964). "Ductility of concrete." *Proc., Int. Symp. on Flexural Mechanics of Reinforced Concrete,* ASCE-ACI, Miami, 213-224.

Schickert, G., and Winkler, H. (1979). "Results of tests concerning strength and strain of concrete subjected to multiaxial compressive stresses." *Deutscher Ausschuss fur Stahlbeton*, Heft 277, Berlin, West Germany.

Scott, B.D., Park, R., and Priestley, M.J.N. (1982). "Stress-strain behavior of concrete confined by overlapping hoops at low and high strain rates." *J. American Concrete Institute,* 79, 13-27.

Shah, S.P., Fafitis, A., and Arnold, R. (1983). "Cyclic Loading of Spirally Reinforced Concrete." *Proceedings ASCE*, 109(7): 1695-1710.

Shama, A.A, and Mander, J.B. (2004). "Behavior of Timber Pile-to-Cap Connections under Cyclic Lateral Loading." *J. Struct. Eng.*, 130(8), 1252-1262.

Sheikh, A., and Yeh, C.C. (1986). "Flexural behaviour of confined concrete columns." *ACI Journal*, 83(3), 389-404.

Thorenfeldt, E., Tomaszewicz, A., and Jensen, J.J. (1987). "Mechanical properties of high-strength concrete and application in design." *Proc. of the Symposium on Utilization of High-Strength Concrete*, Tapir, Trondheim, Norway, 149-159.

Tsai, W.T. (1988). "Uniaxial compression stress-strain relation of concrete." *J. Struct. Eng.*, 114(9), 2133-2136.

Whitney, C.S. (1942). "Plastic theory of reinforced concrete design." *Proceedings ASCE, Transactions ASCE,* 107, 251-326.

William, K.J., and Warnke, E.P. (1975). "Constitutive model for the triaxial behavior of concrete." *Proc., International Association for Bridge and Structural Engineering*, Proceedings, 19, 1-30.

Yong, Y.K., Nour, M.G., Nawy, E.G. (1989). " Behavior of laterally confined high-strength concrete under axial loads.", *J. Struct. Eng.*, 114(2), 332-351.

APPENDIX I

STRESS-STRAIN RELATION FOR UNCONFINED CONCRETE OF DIFFERENT COMPRESSIVE STRENGTHS

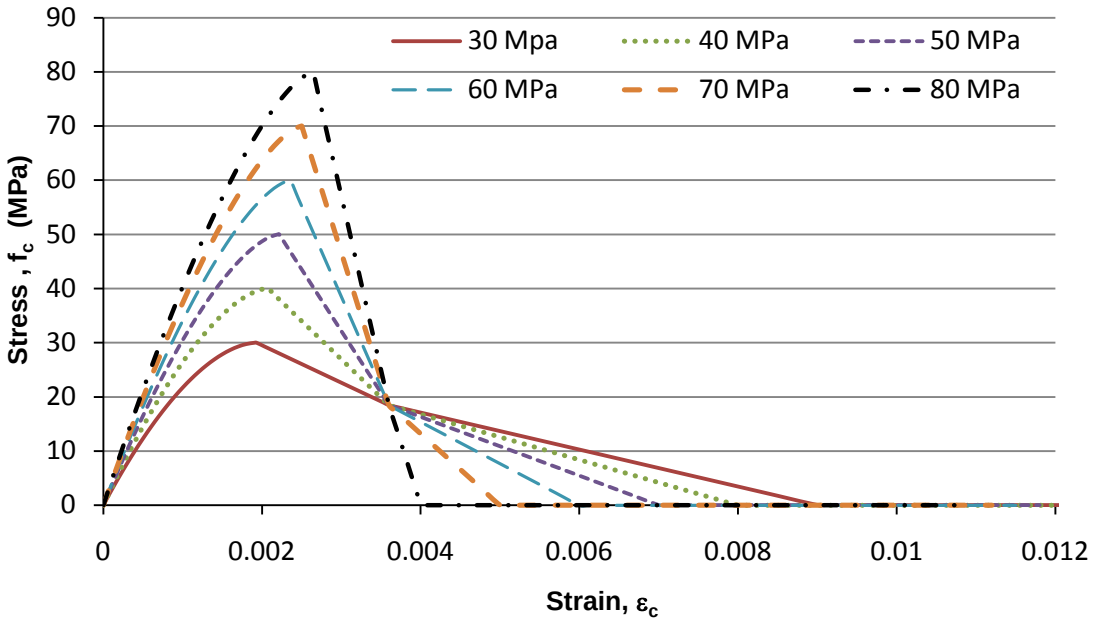

Figure 15: Stress-strain relation for unconfined concrete for various concrete compressive strengths.

APPENDIX II

STRESS-STRAIN RELATION FOR CONFINED CONCRETE OF DIFFERENT COMPRESSIVE STRENGTHS

a. $f_c' = 30\ MPa$

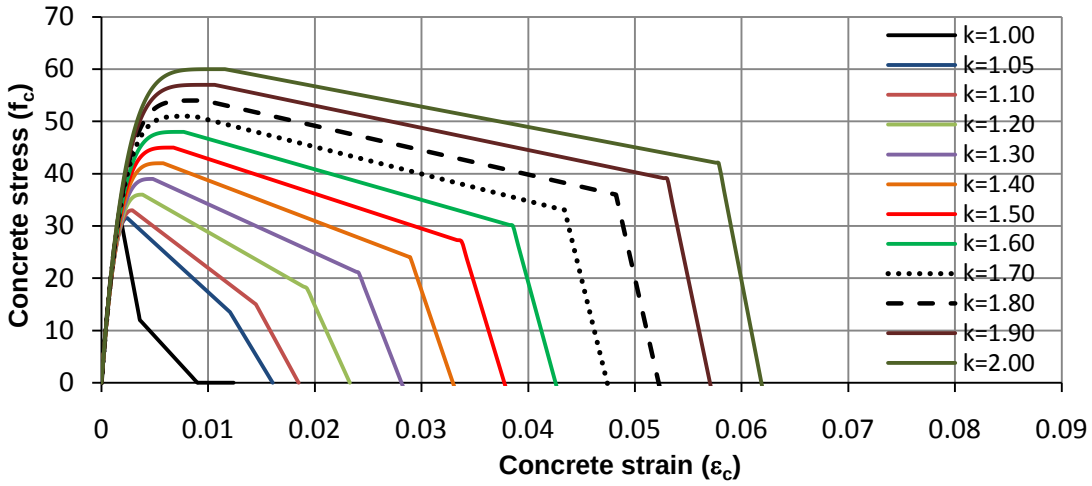

b. $f_c' = 40\ MPa$

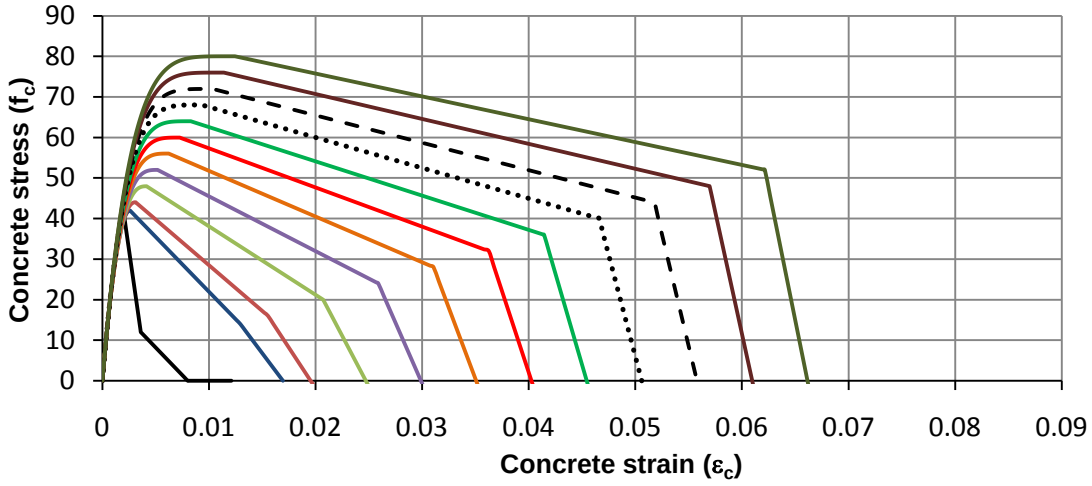

Figure 16: Stress-strain relation for confined concrete for various concrete compressive strengths.

c. $f_c' = 60\ MPa$

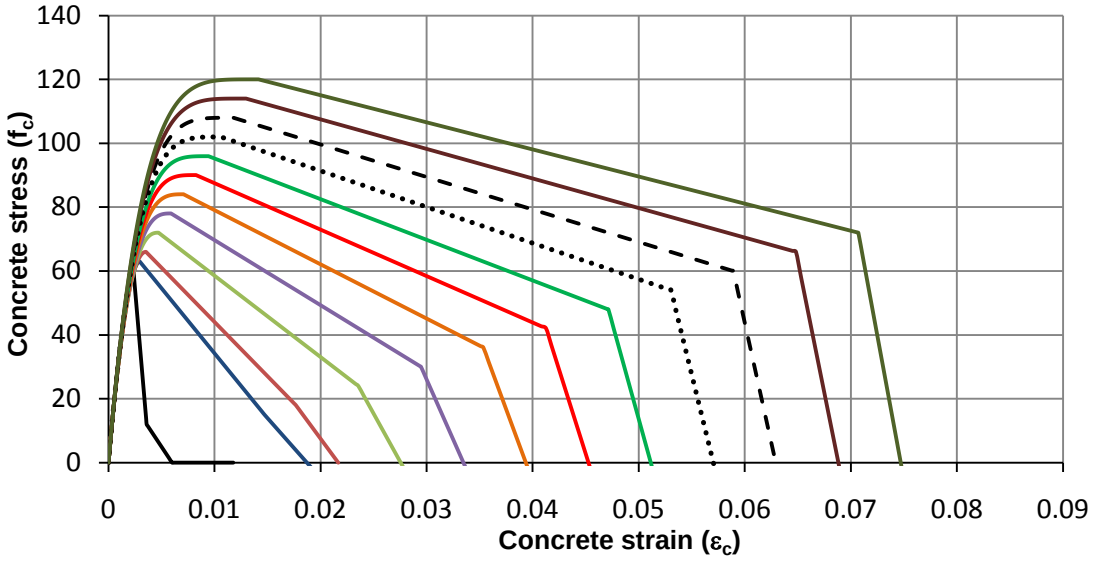

d. $f_c' = 80\ MPa$

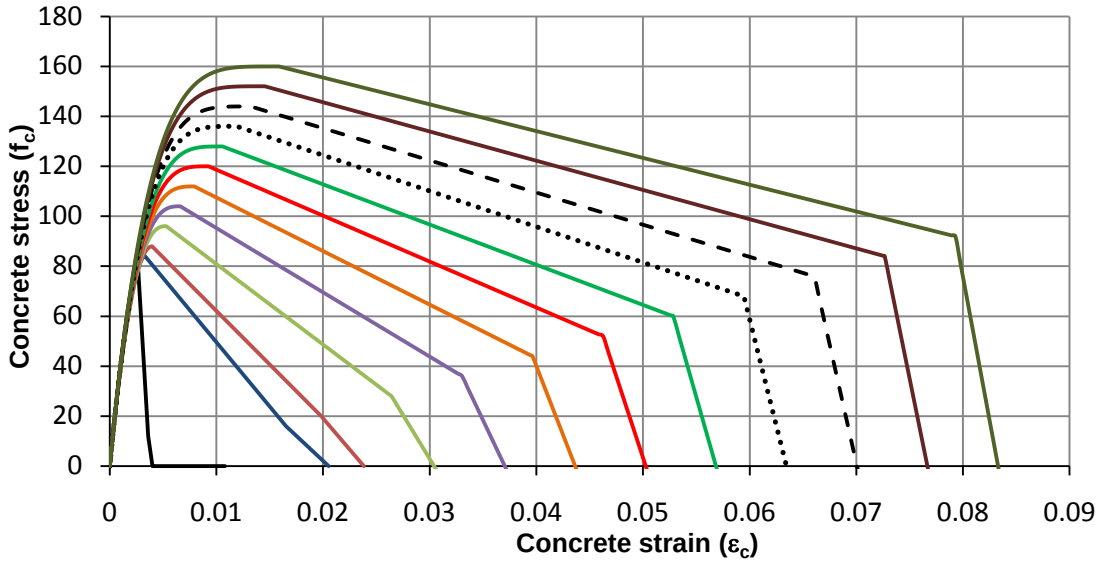

Figure 16 (continued)

APPENDIX III

MATLAB PROGRAM FOR MOMENT-CURVATURE RELATION USING FIBER ANALYSIS

(filename mainprogram.m)

```
%MAIN FUNCTION
clear all;clc;
input_par;   % Function call for input parameters
[splotPhi,splotM]=momentcurvature(); % Function call for moment-curvature analysis
 % Plotting moment-curvature results
 figure;
 plot(splotPhi,splotM,'LineWidth',2)
 title('MOMENT CURVATURE');
 xlabel ('CURVATURE (1/mm)');
 ylabel ('MOMENT (kN-m));
 grid on
```

(filename input_par.m)

```
function [] = input_par()
%FUNCTION TO GET THE INPUT PARAMETERS FROM THE USER
%Declaring the global variables
global vAst vfy vesh vEsh vfsu vesu h b fc eco espall clearcover
      nosteellayer Es diastirrup Ptarget nstrip K cvdt nobarperlayer
      vAst vfy vesh vEsh vfsu vesu Pp vdt Ec n fcc ecc nc
      stirrupspacing ecu
      % Input parameters
```

```
% Section properties

h = input('Enter the height of the section (mm): ');

b = input('Enter the breadth of the section (mm): ');

clearcover = input('Enter the clearcover of the section (mm): ');

Ptarget = input('Enter the target axial load (kN): ');

% Concrete properties

fc = input('Enter unconfined concrete strength (MPa): ');

fcc = input('Enter confined concrete strength (MPa): ');

% Reinforcing steel properties

Es = input('Enter modulus of elasticity of steel (MPa): ');

fy = input('Enter yield strength of reinforcing steel (MPa): ');

esh = input('Enter strain hardening strain: ');

Esh = input('Enter strain hardening modulus (MPa): ');

fsu = input('Enter ultimate strength of steel (MPa): ');

esu = input('Enter ultimate steel strain: ');

bardia = input('Enter longitudinal reinforcing bar diameter (mm):
                                                        ');

nosteellayer = input('Enter number of layers of longitudinal
                                                reinforcing steel: ');
%Loop to get number of longitudinal bars in each layer of steel

for i=1:nosteellayer

      fprintf('INPUT FOR LAYER %d OF STEEL \n \n', i)

      nobarperlayer (i,1) = input('Enter the number of bars in
                                  this layer of steel: ');

      vAst (i,1) = nobarperlayer (i,1)*(pi*bardia (i)^2)/4;

      vfy (i,1) = fy;

      vesh (i,1)= esh;

      vEsh (i,1)= Esh;

      vfsu (i,1)= fsu;

      vesu (i,1)= esu;
```

```
            Pp (i,1) = vEsh(i,1) * (vesu(i,1) - vesh(i,1)) / (vfsu(i,1)
                                                        - vfy(i,1));
      end
      % Loop to calculate the distance to the steel layers from centroidal line
      for i=1:nosteellayer
            disttb = h-2*clearcover-2*diastirrup-0.5*bardia (1,1)-
                     0.5*bardia (nosteellayer,1);
            vdt (i,1) = (clearcover+diastirrup +bardia (1,1)/2 + (i-
                     1)*disttb/ (nosteellayer-1));
            cvdt (i,1) = vdt(i,1)-h/2;
      end
      diastirrup = input('Enter diameter of stirrups (mm): ');
      stirrupspacing = input('Enter stirrup spacing (mm): ');
      %Calculating concrete properties
      Ec = 5000*sqrt(fc);
      eco=0.0015+fc/70000;
      espall =.012-.0001*fc;
      K=fcc/fc;
      ecc =eco*(1+5*(K-1));ecu=5*ecc;
      n=Ec*eco/fc;
      nc=Ec*ecc/fcc;
      nstrip=50; % Total number of strips
```

(filename:momentcurvature.m)

```
function [tempsplotPhi,tempsplotM] = momentcurvature()
%FUNCTION TO DO PERFORM THE MOMENT CURVATURE ANALYSIS
%Declaring the global variables
global Ptarget Ec b h  Es vAst vfy cvdt nstrip ecc estrip hstrip eo phi
      stopmphi diastirrup clearcover
      % Initial assumptions to start the moment curvature analysis
```

```
P(1,1)=0; delPhi = 0; tempsplotPhi(1,1)=0; tempsplotM(1,1)=0;
stopmphi = 0;
eo(1,1) = Ptarget/(10*(Ec*b*h)+ Es*sum(vAst));
% Initial assumption of centroidal strain
phi(1,1) = .000000001*h; % Initial assumption of curvature
s=1; r=1;
hstrip = (h-2*clearcover-diastirrup)/(nstrip-8);
%Start moment curvature analysis
while (stopmphi~=1)
      eo(s,1) = eo(r,1);
      if Ptarget == 0
            deltaP = 1000;
      else
            deltaP = Ptarget; % to get into the while loop the first time
      end
while (abs(deltaP) > (0.0005*vfy'*vAst)/1000)
      %Function call to calculate steel stresses
       [esteel,steelstress] = steelstresses(r,s);
      %  Function call to calculate unconfined and confined concrete stresses
      [uconcstress unAstrip conconcstress conAstrip ystrip] =
                concretestresses(r,s);
      P(s,1) = (steelstress'*vAst + uconcstress'* unAstrip +
             conconcstress'* conAstrip)/1000; % Total forces
      deltaP = -Ptarget - P(s,1);
      if (r==1) && (s==1)
            deltaeo = deltaP/((Ec*b*h)+ Es*sum(vAst));
      else
            delP = (P(s,1)-P(s-1,1));
```

```
            deleo = (eo(s,1)-eo(s-1,1));
            deltaeo = deltaP/(delP / deleo);
            if deleo == 0
                  deltaeo = deltaP/((Ec*b*h)+ Es*sum(vAst));
            end
      end
      eo(s+1,1) = eo(s,1) + deltaeo;
      s=s+1;
end
% Stop the moment-curvature analysis when core concrete fails
if (abs(estrip(5,1)) > 5*ecc || abs(estrip(46,1))> 5*ecc)
      fprintf ('Core concrete failed');
      stopmphi=1;
      break;
end
tempsplotPhi(r+1,1) = phi(r,1);
tempsplotM(r+1,1) = (steelstress'*(vAst.*cvdt)+
                     uconcstress'*(unAstrip.*ystrip) +
                     conconcstress'*(conAstrip.*ystrip))/1000000;
if (r>=1 && r<=20)
      deltaPhi = .0001/h;
elseif (r>20 && r<=50)
      deltaPhi = .0002/h;
else
      deltaPhi = .0005/h;
end
r=r+1;
phi(r,1) = phi(r-1,1)+deltaPhi;
delPhi = phi(r,1) - phi(r-1,1);
deltaeo = (deltaP - (delP/delPhi)*deltaPhi)/(delP/deleo);
```

```
      eo(r,1) = eo(r,1) + deltaeo;
      end
```

(filename:steelstress.m)

```
function [esteel,steelstress] = steelstresses(tr,ts)
%FUNCTION TO CALCULATE THE STEEL STRESSES
%Declaring the global variables
global nosteellayer eo phi cvdt Es vfy vfsu vesu Pp vesh
      esteel=[];steelstress=[];
      for q = 1:nosteellayer
            esteel(q,1) = eo(ts,1) + phi(tr,1) * cvdt(q,1);
            if (esteel(q,1))>0
            steelstress(q,1) =
                    ((Es*abs(esteel(q,1))/(1+abs(Es*esteel(q,1) /
                    vfy(q,1))^20)^0.05) + (vfsu(q,1)-vfy(q,1))*(1 -
                    ((abs(vesu(q,1)-abs(esteel(q,1)))) ^Pp(q,1)/
                    (((abs(vesu(q,1)-vesh(q,1)))^(20*Pp(q,1)))+
                    ((abs(vesu(q,1)-abs(esteel(q,1))))
                    ^(20*Pp(q,1))))^0.05)));
            elseif (esteel(q,1))<0
            steelstress(q,1) =  -
                     (((Es*abs(esteel(q,1))/(1+abs(Es*esteel(q,1) /
                     vfy(q,1))^20)^0.05)+ (vfsu(q,1)-vfy(q,1))*(1 -
                     ((abs(vesu(q,1)-abs(esteel(q,1))))^Pp(q,1)/
                     (((abs(vesu(q,1) –
                     vesh(q,1)))^(20*Pp(q,1)))+ ((abs(vesu(q,1)-
                     abs(esteel(q,1))))
                     ^(20*Pp(q,1))))^0.05))));
            end
      end
```

(filename:concretestresses.m)

```
function[tuconcstress tunAstrip tconconcstress tconAstrip
        tystrip]=concretestresses(tr,ts)
%FUNCTION TO CALCULATE THE CONCRETE STRESS - BOTH CONFINED AND
UNCONFINED
global b h  fc n eco espall hstrip nstrip diastirrup clearcover fcc ecc
     nc estrip eo phi K estripext confestripext
    % Parameters for proposed concrete stress-strain model
      ec1=0.0036;fc1=12;
      ecu=5*ecc; % Hoop fracture strain
      fcu=12+fc*(K-1);
      ef=ecu+0.004;
      Eppu = (fc1-fc)/(ec1-eco);
      Eppc = (fcu-fcc)/(ecu-ecc);
      z = h/(2*nstrip); %distance to the center of the first strip from the top
      tystrip=[];estrip=[];tuconcstress=[]; tunAstrip=[];
      tconconcstress=[]; tconAstrip=[];
      for w=1:nstrip
      %distance to the center of the strip from the  neutral axis
         tystrip(w,1) = -(h/2-z);
         if w<=5
            tystrip(1,1) = -(h/2-((clearcover+diastirrup/2)/4)/2);
            tystrip(2,1) = tystrip(1,1)+ (clearcover+diastirrup/2)/4;
            tystrip(3,1) = tystrip(2,1)+ (clearcover+diastirrup/2)/4;
            tystrip(4,1) = tystrip(3,1)+ (clearcover+diastirrup/2)/4;
            tystrip(5,1) = -((h/2-(clearcover+diastirrup/2))-hstrip/2);
         end
```

```
   if w>5 && w<nstrip-3
            tystrip(w,1) = tystrip(5,1)+ (w-5)*hstrip;
   end
   if w>=(nstrip-3)
      tystrip(47,1)=-tystrip(4,1);
      tystrip(48,1)=-tystrip(3,1);
      tystrip(49,1)=-tystrip(2,1);
      tystrip(50,1)=-tystrip(1,1);
   end
estripext = eo(ts,1) + phi(tr,1)*exfibdist;
confestripext = eo(ts,1) + phi(tr,1)* confexfibdist;
estrip(w,1) = eo(ts,1) + phi(tr,1)* tystrip(w,1);
tuconcstress(w,1)=0; tunAstrip(w,1)=0; tconconcstress(w,1)=0;
tconAstrip(w,1)=0;
if w == 1 || w == 2 || w==3 || w==4 || w == nstrip-3 || w ==
                       nstrip-2 || w == nstrip-1 || w == nstrip
tunAstrip(w,1) = ((clearcover+diastirrup/2)/4)*b;
%Calculation of unconfined concrete stresses
if estrip(w,1)<0
      if abs(estrip(w,1))<eco
          tuconcstress(w,1)=-(fc*(1-abs(1-
                                    abs(estrip(w,1))/eco)^n));
      elseif abs(estrip(w,1))>=eco && abs(estrip(w,1))<ec1
            tuconcstress(w,1)=-(fc+Eppu*(abs(estrip(w,1))-eco));
      elseif abs(estrip(w,1))>=ec1 && abs(estrip(w,1))<espall
            tuconcstress(w,1)=-(fc1*(espall-abs(estrip(w,1)))/
                                          (espall-ec1));
      elseif abs(estrip(w,1))>=espall
            tuconcstress(w,1)=0;
      end
```

```
else
      tuconcstress(w,1)=0;
end
else
%Calculation of confined concrete stresses
buncon=2*(clearcover+diastirrup/2); %Breadth of the unconfined portion
                                    of concrete
bcon=b-buncon;
tconAstrip(w,1)=hstrip*bcon; tunAstrip(w,1) = hstrip*buncon;
if(estrip(w,1)<0)
      if abs(estrip(w,1))<eco
            tuconcstress(w,1)=-(fc*(1-abs(1-
                                    abs(estrip(w,1))/eco)^n));
      elseif abs(estrip(w,1))>=eco && abs(estrip(w,1))<ec1
            tuconcstress(w,1)=-(fc+Eppu*(abs(estrip(w,1))-eco));
      elseif abs(estrip(w,1))>=ec1 && abs(estrip(w,1))<espall
            tuconcstress(w,1)=-(fc1*(espall-abs(estrip(w,1)))/
                                    (espall-ec1));
      elseif abs(estrip(w,1))>=espall
            tuconcstress(w,1)=0;
      end
      if abs(estrip(w,1))<ecc
            tconconcstress(w,1) = -(fcc*(1-abs(1-abs(estrip(w,1))
                                    /ecc)^nc));
      elseif abs(estrip(w,1))>=ecc && abs(estrip(w,1))<ecu
            tconconcstress(w,1) = -(fcc + Eppc*(abs(estrip(w,1))-
                                    ecc));
      elseif abs(estrip(w,1))>=ecu && abs(estrip(w,1))<ef
            tconconcstress(w,1) = -(fcu*(ef-abs(estrip(w,1)))/
                                    (ef-ecu));
```

```
            elseif abs(estrip(w,1))>ef
                  tconconcstress(w,1) =0;
            end
      else
            tuconcstress(w,1)=0;
            tconconcstress(w,1)=0;
      end
      end
      z=z+hstrip;
      end
```

MATLAB PROGRAM FOR THE COMPUTATIONAL STRESS-BLOCK BASED MOMENT-CURVATURE ANALYSIS

```
clear all; clc;
h = input('Enter the height of the section (mm): ');
b = input('Enter the breadth of the section (mm): ');
clearcover = input('Enter the clearcover of the section (mm): ');
Ptarget = input('Enter the target axial load (kN): ');
% Concrete properties
fc = input('Enter unconfined concrete strength (MPa): ');
fcc = input('Enter confined concrete strength (MPa): ');
ec1=0.0036;fc1=12;
ecu=5*ecc;ef=ecu+0.004;
fcu=12+fc*(K-1);
n=Ec*eco/fc;
nc=Ec*ecc/fcc;
% Reinforcing steel properties
Es = input('Enter modulus of elasticity of steel (MPa): ');
```

```
fy = input('Enter yield strength of reinforcing steel (MPa): ');
esh = input('Enter strain hardenig strain: ');
Esh = input('Enter strain hardening modulus (MPa): ');
fsu = input('Enter ultimate strength of steel (MPa): ');
esu = input('Enter ultimate steel strain: ');
bardia = input('Enter longitudinal reinforcing bar diameter (mm): ');
diastirrup = input('Enter diameter of stirrups (mm): ');
stirrupspacing = input('Enter stirrup spacing (mm): ');
dAst1 = input('Enter centroidal distance to layer 1 of steel(mm): ');
dAst2 = input('Enter centroidal distance to layer 2 of steel(mm): ');
dAst3 = input('Enter centroidal distance to layer 3 of steel(mm): ');
dAst4 = input('Enter centroidal distance to layer 4 of steel(mm): ');
Ast1 = 4*pi()*dia^2/4;
Ast4 = Ast1;
Ast2 = 2*pi()*dia^2/4;
Ast3=Ast2;
Pp = Esh*(esu-esh)/(fsu-fy);
%Calculating concrete properties
Ec = 5000*sqrt(fc);
eco=0.0015+fc/70000;
espall =.012-.0001*fc;
K=fcc/fc;
ecc =eco*(1+5*(K-1));ecu=5*ecc;
n=Ec*eco/fc;
nc=Ec*ecc/fcc;
% Values for first iteration
P(1)=0;
plotM(1)=0;
PlotPhi(1)=0;
delPhi = 0;
```

```
eo(1) = Ptarget/(10*(Ec*b*h)+ Es*Ast1+Ast2+Ast3+Ast4);
phi(1) = .000000001*h + delPhi;
for i=1:300
      deltaP = 10;    %for the while loop to take place the first time
      j=2;
      while (abs(deltaP) > 1)
      confexfibdist = -(h/2-(clearcover+diastirrup/2));
      estripext = eo(j-1) + phi(i) * -(h/2);
      confestripext = eo(j-1) + phi(i) * confexfibdist;
      steelstrain1 = eo(j-1) + phi(i) * dAst1;
      steelstrain2 = eo(j-1) + phi(i) * dAst2;
      steelstrain3 = eo(j-1) + phi(i) * dAst3;
      steelstrain4 = eo(j-1) + phi(i) * dAst4;
      %Stresses in steel
      if steelstrain1 < 0
      steelstress1 = -((Es*abs(steelstrain1)/(1+abs(Es*steelstrain1/fy)
                     ^20)^0.05)+(fsu-fy)*(1-(abs(esu-abs(steelstrain1))
                     ^Pp/(abs(esu-esh)^(20*Pp)+abs(esu-
                     abs(steelstrain1))^(20*Pp))^0.05)));
      else
      steelstress1 = ((Es*abs(steelstrain1)/(1+abs(Es*steelstrain1/fy)
                     ^20)^0.05)+(fsu-fy)*(1-(abs(esu-abs(steelstrain1))
                     ^Pp/ (abs(esu-esh)^(20*Pp)+abs(esu-
                     abs(steelstrain1))^ (20*Pp))^0.05)));
      end
      if steelstrain2 < 0
      steelstress2 = -((Es*abs(steelstrain2)/(1+abs(Es*steelstrain2/fy)
                     ^20)^0.05)+(fsu-fy)*(1-(abs(esu-abs(steelstrain2))
                     ^Pp/(abs(esu-esh)^(20*Pp) +abs(esu-
                     abs(steelstrain2))^ (20*Pp))^0.05)));
```

```
        else
        steelstress2 = ((Es*abs(steelstrain2)/(1+abs(Es*steelstrain2/fy)
                       ^20)^0.05)+(fsu-fy)*(1-(abs(esu-abs(steelstrain2))
                       ^Pp/ (abs(esu-esh)^(20*Pp) +abs(esu-
                       abs(steelstrain2))^ (20*Pp))^0.05)));
        end
        if steelstrain3 < 0
        steelstress3 = -((Es*abs(steelstrain3)/(1+abs(Es*steelstrain3/fy)
                       ^20)^0.05)+(fsu-fy)*(1-(abs(esu-abs(steelstrain3))
                       ^Pp/ (abs(esu-esh)^(20*Pp) + abs(esu-
                       abs(steelstrain3))^ (20*Pp))^0.05)));
        else
        steelstress3 = ((Es*abs(steelstrain3)/(1+abs(Es*steelstrain3/fy)
                       ^20)^0.05)+(fsu-fy)*(1-(abs(esu-abs(steelstrain3))
                       ^Pp/ (abs(esu-esh)^(20*Pp) +abs(esu-
                       abs(steelstrain3))^ (20*Pp))^0.05)));
        end
        if steelstrain4 < 0
        steelstress4 = -((Es*abs(steelstrain4)/(1+abs(Es*steelstrain4/fy)
                       ^20)^0.05)+(fsu-fy)*(1-(abs(esu-abs(steelstrain4))
                       ^Pp/ (abs(esu-esh)^(20*Pp) +abs(esu-
                       abs(steelstrain4))^ (20*Pp))^0.05)));
        else
        steelstress4 = ((Es*abs(steelstrain4)/(1+abs(Es*steelstrain4/fy)
                       ^20)^0.05)+(fsu-fy)*(1-(abs(esu-abs(steelstrain4))
                       ^Pp/(abs(esu-esh)^(20*Pp) +abs(esu-
                       abs(steelstrain4))^(20*Pp))^0.05)));
        end
steelforce1 = steelstress1*Ast1;
steelforce2 = steelstress2*Ast2;
steelforce3 = steelstress3*Ast3;
```

```
steelforce4 = steelstress4*Ast4;
neutral = estripext / phi(i);
if confestripext<=espall
      estripcore=confestripext;
else
      neutralx = (abs(neutral)-(clearcover+diastirrup/2))*espall/
                                                      confestripext;
      estripcore = eo(j-1) + phi * -abs(neutralx);
end
xc = abs(estripext)/eco;
xu = ec1/eco;
%Stress-block parameters for unconfined concrete
if abs(estripext)<eco
      alphabeta = 1+((1-xc)^(n+1)-1)/(xc*(n+1));
      beta = 2-2/(xc^2*alphabeta)*(xc^2/2+xc*(1-xc)^(n+1)/(n+1)+((1-
             xc)^(n+2)-1)/((n+1)*(n+2)));
      alpha = alphabeta/beta;
elseif abs(estripext)>=eco && abs(estripext)<ec1
      alphabeta = n/(xc*(n+1))+(1-1/xc)*(1+(12-fc)*(xc-1)/(2*fc*(xu-
                                                          1)));
      beta = 2-1/(xc^2*alphabeta)*(n*(n+3)/((n+1)*(n+2))+(xc^2-1)+(12-
             fc)*(2*xc^3-3*xc^2+1)/(3*fc*(xu-1)));
      alpha = alphabeta/beta;
elseif abs(estripext)>=ec1 && abs(estripext)<espall
      alphabeta = n/(xc*(n+1))+(ec1-eco)/abs(estripext)*((12+fc)/
                  (2*fc))+fc1*(1-ec1/abs(estripext))*
                  (abs(estripext)+ec1-2*espall)/(2*fc*(ec1-espall));
      beta = 2-1/(xc^2*alphabeta)*(n*(n+3)/((n+1)*(n+2))+(xu^2-1)+(12-
             fc)*(2*xu^3-3*xu^2+1)/(3*fc*(xu-1))+fc1* (abs(estripext)-
             ec1)*(2*(abs(estripext)^2+ abs(estripext)*ec1+ec1^2)-
```

```
            3*espall*(abs(estripext)+ec1)) /(3*fc*eco^2*(ec1-
            espall)));
      alpha = alphabeta/beta;
elseif abs(estripext)>=espall
      alphabeta = n/(xc*(n+1))+(ec1-eco)/abs(estripext)*((12+fc)/
                  (2*fc))+fc1*(espall-ec1)/(2*fc*abs(estripext));
      beta = 2-1/(xc^2*alphabeta)*(n*(n+3)/((n+1)*(n+2))+(xu^2-1)+(12-
             fc)*(2*xu^3-3*xu^2+1)/(3*fc*(xu-1))+fc1*(2*ec1^3+espall^3-
             3*espall*ec1^2)/(3*fc*eco^2*(espall-ec1)));
      alpha = alphabeta/beta;
end
xc1 = abs(estripcore)/eco;
xu1 = ec1/eco;
if abs(estripcore)<eco
      alphabeta1 = 1+((1-xc1)^(n+1)-1)/(xc1*(n+1));
      beta1 = 2-2/(xc1^2*alphabeta1)*(xc1^2/2+xc1*(1-xc1)
              ^(n+1)/(n+1)+((1-xc1)^(n+2)-1)/((n+1)*(n+2)));
      alpha1 = alphabeta1/beta1;
elseif abs(estripcore)>=eco && abs(estripcore)<ec1
      alphabeta1 = n/(xc1*(n+1))+(1-1/xc1)*(1+(12-fc)*(xc1-
                   1)/(2*fc*(xu1-1)));
      beta1 = 2-1/(xc1^2*alphabeta1)*(n*(n+3)/((n+1)*(n+2))+(xc1^2-
              1)+(12-fc)*(2*xc1^3-3*xc1^2+1)/(3*fc*(xu1-1)));
      alpha1 = alphabeta1/beta1;
elseif abs(estripcore)>=ec1 && abs(estripcore)<espall
      alphabeta1 = n/(xc1*(n+1))+(ec1-eco)/abs(estripcore)*((12+fc)/
                   (2*fc))+fc1*(1-ec1/abs(estripcore))*
                   (abs(estripcore)+ec1-2*espall)/(2*fc*(ec1-espall));
      beta1 = 2-1/(xc1^2*alphabeta1)*(n*(n+3)/((n+1)*(n+2))+(xu1^2-
             1)+(12-fc)*(2*xu1^3-3*xu1^2+1)/(3*fc*(xu1-1))+fc1*
             (abs(estripcore)-ec1)*(2*(abs(estripcore)^2+
```

```
            abs(estripcore)*ec1+ec1^2)-3*espall*(abs(estripcore)+ec1))
            /(3*fc*eco^2*(ec1-espall)));
      alpha1 = alphabeta1/beta1;
elseif abs(estripcore)>=espall
      alphabeta1 = n/(xc1*(n+1))+(ec1-eco)/abs(estripcore)*((12+fc)
                  /(2*fc))+ fc1*(espall-ec1)/(2*fc*abs(estripcore));
      beta1 = 2-1/(xc1^2*alphabeta1)*(n*(n+3)/((n+1)*(n+2))+(xu1^2-
              1)+(12-fc)*(2*xu1^3-3*xu1^2+1)/(3*fc*(xu1-1))+fc1*
              (2*ec1^3+espall^3-3*espall*ec1^2)/(3*fc*eco^2*(espall-
              ec1)));
      alpha1 = alphabeta1/beta1;
end
xcc = abs(confestripext)/ecc;
xuc =ecu/ecc;
%Stress-block parameters for confined concrete
if abs(confestripext)<ecc
      alphabetacc = 1+((1-xcc)^(nc+1)-1)/(xcc*(nc+1));
      betacc = 2-2/(xcc^2*alphabetacc)*(xcc^2/2+xcc*(1-xcc)^(nc+1)/
               (nc+1)+((1-xcc)^(nc+2)-1)/((nc+1)*(nc+2)));
      alphacc = alphabetacc/betacc;
elseif abs(confestripext)>=ecc && abs(confestripext)<ecu
      alphabetacc = nc/(xcc*(nc+1))+(1-1/xcc)*(1+(12-fc)*(xcc-
                    1)/(2*fc*(xuc-1)));
      betacc = 2-1/(xcc^2*alphabetacc)*(nc*(nc+3)/((nc+1)*(nc+2))+
              (xcc^2-1)+(12-fc)*(2*xcc^3-3*xcc^2+1)/(3*fc*(xuc-1)));
      alphacc = alphabetacc/betacc;
elseif abs(confestripext)>=ecu && abs(confestripext)<ef
     alphabetacc = nc/(xcc*(nc+1))+(ecu-ecc)/abs(confestripext)*
                   ((12+fc)/(2*fc))+fcu*(1-ecu/abs(confestripext))
                   *(abs(confestripext) +ecu-2*ef)/(2*fc*(ecu-ef));
```

```
      betacc = 2-1/(xcc^2*alphabetacc)*(nc*(nc+3)/((nc+1)*(nc+2))
             +(xuc^2-1)+(12-fc)*(2*xuc^3-3*xuc^2+1)/(3*fc*(xuc-
             1))+fcu*(abs(confestripext)-ecu)*(2*(abs(confestripext)^2
             +abs(confestripext)*ecu+ecu^2)-3*ef*(abs(confestripext)
             +ecu))/(3*fc*ecc^2*(ecu-ef)));
      alphacc = alphabetacc/betacc;
elseif abs(confestripext)>=ef
      alphabetacc = nc/(xcc*(nc+1))+(ecu-ecc)/abs(confestripext)*
                  ((12+fc)/(2*fc)) +fcu*(ef-ecu)/(2*fc*
                  abs(confestripext));
      betacc = 2-1/(xcc^2*alphabetacc)*(nc*(nc+3)/((nc+1)*(nc+2))+
             (xuc^2-1)+(12-fc)*(2*xuc^3-3*xuc^2+1)/(3*fc*(xuc-1))
             +fcu*(2*ecu^3+ef^3-3*ef*ecu^2)/(3*fc*ecc^2*(ef-ecu)));
      alphacc = alphabetacc/betacc;
end
totunconforce =-((alpha*fc*beta*abs(neutral)*b));
subunconforce = (alpha1*fc*beta1*(abs(neutral)-(clearcover
              +diastirrup/2))*(b-2*(clearcover+diastirrup/2)));
unconforce = totunconforce + subunconforce ;
confconforce = -((alphacc*fcc*betacc*(abs(neutral)-(clearcover
              +diastirrup/2))*(b-2*(clearcover+diastirrup/2))));
P(j)= (steelforce1 + steelforce2 + steelforce3 +steelforce4 +
       unconforce + confconforce)/1000;
deltaP = -Ptarget-P(j);
if (j==2)
      deltaeo = deltaP/((Ec*b*h)+ Es*(Ast1+Ast2+Ast3+Ast4));
else
      delP = (P(j)-P(j-1));
      deleo = (eo(j-1)-eo(j-2));
      deltaeo = deltaP/(delP / deleo);
end
```

```
      eo(j) = eo(j-1) + deltaeo;
      j=j+1;
end
plotM(i) = (steelforce1*dAst1 + steelforce2*dAst2 + steelforce3*dAst3 +
         steelforce4*dAst4 + totunconforce*(-(h/2-
         beta*abs(neutral)/2))+ subunconforce *(-(h/2-
         (clearcover+diastirrup/2)-beta1/2*(abs(neutral)-
         (clearcover+diastirrup/2)))) + confconforce*(-(h/2-
         (clearcover+diastirrup/2)-betacc*(abs(neutral)-
         (clearcover+diastirrup/2))/2)))/1000000;
plotPhi(i) = phi(i);
if (i>=1 && i<=20)
      deltaPhi = .0001/h;
elseif (i>20 && i<=50)
      deltaPhi = .0002/h;
else
      deltaPhi = .0005/h;
end
phi(i+1) = phi(i)+deltaPhi;
if i==1
      delPhi = phi(i);
else
      delPhi = phi(i) - phi(i-1);
end
deltaeo = (deltaP - (delP/delPhi)*deltaPhi)/(delP/deleo);
tempeo = eo(j-1) + deltaeo;
eo=[];P=[];
eo(1)=tempeo;
end
% Moment Curvature Plot
```

```
plot(plotPhi, plotM)
title('MOMENT CURVATURE);
xlabel(‘CURVATURE (1/mm)')
ylabel(‘MOMENT (kN-m)')
grid on
```

VITA

Madhu Karthik Murugesan Reddiar received his Bachelor of Technology degree from Pondicherry University, Puducherry, India in May of 2005. He entered the Structural Engineering program at Texas A&M University in January 2008 and received his Master of Science degree in December 2009.

Mr. Madhu may be reached at CE/TTI, 709-E, 3136 TAMU, College Station, TX 77843-3136, USA. His email is madhukarthik11@gmail.com.